Title
Controlled fabrication of patternable conductive hydrogels and their properties

Author
Cardenas, Anne Marie

Publication Date
2022

Peer reviewed|Thesis/dissertation

UNIVERSITY OF CALIFORNIA

Los Angeles

Controlled fabrication of patternable conductive hydrogels and their properties

A thesis submitted in partial satisfaction

of the requirements for the degree Master of Science

in Materials Science and Engineering

by

Anne Marie Cardenas

2022

ABSTRACT OF THE THESIS

Controlled fabrication of patternable conductive hydrogels and their properties

by

Anne Marie Cardenas

Master of Science in Materials Science and Engineering

University of California, Los Angeles, 2022

Professor Ximin He, Chair

Stretchable and conductive hydrogels compatible with 3D printing techniques are of critical importance for electronics applications. A wide range of mechanical properties are desired with specific ranges required for different devices such as soft and tissue-like mechanical properties for applications relating to the human body and stronger mechanical properties for applications in soft robotics. Ease of fabrication to obtain complex configurations is a desirable trait for these materials. However, being able to quickly pattern them while still maintaining a high degree of electrical conductivity and stretchability is often hard to achieve. Here we developed UV-crosslinkable hydrogels that can reach high electronic conductivity (>10 S/m) and good stretchability (>150%) based on the combination of poly(3,4-ethylenedioxythiophene): polystyrene sulfonate (PEDOT:PSS), ionic liquid, and a hydrogel matrix.

In Chapter 1 the fundamentals of conductive hydrogels are discussed. In Chapter 2 the work done to obtain a 3D printable conductive hydrogel with tissue-like mechanical properties (1-

100 kPa) is presented. In brief, a polyacrylamide hydrogel matrix is employed and exhibits soft mechanical properties in addition to working in conjunction with the PEDOT:PSS to obtain high electronic conductivities. The resulting material is UV-crosslinkable and achieved in a one-pot synthesis method, capable of producing complex 2D and 3D structures by digital light processing (DLP) printing. In Chapter 3 A poly(vinyl alcohol) methacrylate is utilized and further strengthened to obtain higher mechanical properties (>1 MPa). The resulting material is also UV-crosslinkable and achieved in a one-pot synthesis method. Future directions are outlined for both works.

The thesis of Anne Marie Cardenas is approved.

Yu Huang

Andrea Kasko

Ximin He, Committee Chair

University of California, Los Angeles

2022

Dedicated to my family and friends

Table of Contents

List of Figures

List of Tables

ACKNOWLEDGEMENTS

First, I would like to acknowledge my advisor Professor Ximin He and my fellow graduate students within the He group. Thank you for the invaluable lessons and for sharing your knowledge with me. Second, I would like to thank Professor Yu Huang and Professor Andrea Kasko for taking the time to serve as my committee members. I would also like to thank my parents, Lucio, and Martha, as well as my brothers, Roberto, and David, for their support. Although it was at a distance, their love and encouragement could be felt each day. Thank you to my family in Los Angeles: my uncle Alfonso, my cousins Claudio and Christa, and my niece, Isla. Your presence and support are what helped me through navigating graduate school during a global pandemic. To my friends and mentors that have been on this journey with me ever since I discovered what graduate school was. Thanks for never giving up on me and for helping me get to where I am today.

Chapter 1: Background

1.1 Conductive hydrogel fundamentals

Hydrogels are three-dimensional (3D) hydrophilic polymer networks which exhibit good biocompatibility [1]. Hydrogels are set apart from other polymer composites by their high-water content. The mass percentage of water is typically higher than the mass percentage of the solid polymer content. This feature allows for high elasticity and soft mechanical properties [2]. Hydrogels can be modified to possess conductive properties with the addition of conductive fillers into their matrix. In nature, conductivity is achieved either through ion or electron transport. Biological systems usually use the flow of ions to transmit electrical information across cells and tissue while inorganic devices rely on the flow of electrons. Hydrogels are versatile in that their conductive properties can derive from both mechanisms depending on the additives and monomers used [1]. Common conductive fillers in hydrogels include salts, metallic nanomaterials, carbon-based materials, and conducting polymers [1]. Each filler has different advantages depending on the target application and desired properties.

Conductive hydrogels have become increasingly more important for the novel properties they can afford to the realms of biomedical devices, wearable sensors, and soft robotics as flexible conductors [1,2,3]. The ability to remain conductive under considerable strain is already a major advantage over traditional rigid electronics, which have a limited dynamic range with less than 5% strain capacity. Conformability and stretchability allow a material to be used in applications that are meant to operate close to human beings due to the dynamic nature in which they interact within their environment [3]. The properties that set conductive hydrogels apart from other flexible conductors is their soft, water-containing, and tunable mechanical properties. Biological tissues

are usually orders of magnitude softer than engineered materials, which tend to be in the GPa modulus range [4, 5]. By contrast, the softest biological tissue, the brain, displays elastic modulus of around 0.5-1 kPa [6] and the stiffest tissues, such as cartilage, display a modulus around 800 kPa [7]. Conductive hydrogels typically display an elastic modulus within this range, making them especially suitable for implantable devices and wearable devices as the mechanical mismatch between the device and biological tissue would be minimal [1]. Other applications such as soft robotics can also benefit from the properties displayed by conductive hydrogels. Utilizing soft components has the potential to make the interactions between robots and humans safer as there is less risk of injury due to accidental impact with rigid components [3]. While this application requires relatively soft components compared to the typical rigid metallic parts used in conventional robotics, the needed elastic modulus in the 1-100 MPa range which is considerably stiffer that the ones displayed by typical hydrogels (0.01-1 MPa) [6,7]. Fortunately, strategies have been developed to strengthen hydrogels to achieve both a higher modulus (1-10 MPa) and elongation (>150%) [9], making these materials suitable for use in actuators and soft robotics, although their demonstration in conjunction with 3D printable systems is still limited. Adapting these strategies into achieving patternable, strong, and conductive hydrogels is therefore of paramount importance.

1.2 Advantages of rapid fabrication procedures

Hydrogels can be formed by cross-linking polymer chains within an aqueous medium either via chemical cross-linking or physical entanglements [2]. Hydrogels which are polymerized via monomers in the presence of crosslinking agents such as heat, radiation and light are considered chemically cross-linked [1]. Hydrogels formed via hydrogen bonding, electrostatic interactions, or

ionic interactions are denominated physically crosslinked hydrogels [1]. A major difference between the two is that chemically crosslinked hydrogels form covalent bonds which are permanent whereas physically crosslinked gels can potentially be reverted [1]. This work utilizes both to realize UV light-crosslinkable and mechanically tunable hydrogels. Typically, conductive hydrogels are formed within molds to obtain patterns or simple structures. While effective and useful for applications requiring mass production, this method can seriously undermine its usability in applications that require customizability and rapid prototyping [2]. 3D printing technology presents as an attractive alternative. By utilizing light-curable hydrogels or extrudable hydrogel inks a wide range of 3D printing techniques such as stereolithography (SL), digital light processing (DLP), inkjet printing, and direct ink write (DIW) can be utilized to achieve complex structures [1]. While these techniques are a quick way to achieve patterns with good spatial resolution, obtaining a conductive hydrogel system that can exhibit a combination of high conductivity, good stretchability, and a crosslinking method compatible with 3D printing techniques simultaneously is still very challenging and is a key aspect that this work attempted to address.

1.3 Conducting polymers and their structure modification

As mentioned above the conductivity in conductive hydrogels is supplied by additives. While many different fillers can be used, conductive polymers are typically preferred due to their biocompatibility and ease of solution processing [1]. Poly(3,4-ethylenedioxythiophene) polystyrene sulfonate (PEDOT:PSS) is often used over other conductive polymers due to its high conductivity [2]. However, mixing it into a hydrogel matrix compromises its conductivity compared to its thin film form as the conductive domains become entangled within the insulating

components and the water content of the hydrogel. Therefore, strategies to increase the innate conductivity of PEDOT:PSS must be employed to offset some of the loss. Common strategies include the use of polar solvents or freeze-dried PEDOT:PSS [9] and both have been employed within conducting hydrogels with moderate success although they have yet to achieve a compromise between good conductivity, stretchability, and printability. An emerging strategy, and the one used in this work is the addition of select ionic liquids. Ionic liquids are salts that contain one ion with a delocalized charge and at least one organic ion. This poor coordination leads to them exhibiting a liquid state at temperatures below 100 °C [10]. A wide range of them have been proven to effectively increase the conductivity via modification of the PEDOT:PSS structure [11]. Their use in conductive hydrogels has been limited thus far, however, they have already proven to surpass the performance of other conductivity enhancement strategies [12]. To our knowledge, they have yet to be used in a UV-crosslinkable conductive hydrogel system.

This work aims to utilize ionic liquids as an additive to enhance the conductivity of PEDOT:PSS and obtain a conductive hydrogel that is UV-crosslinkable and stretchable. Two different hydrogel matrix systems are explored to achieve different mechanical properties. In Chapter 2 polyacrylamide (PAAm) is employed to target elastic modulus within biologically relevant tissue ranges (5-100 kPa). In Chapter 3 poly(vinyl alcohol)-methacrylate (PVA) is paired with physical crosslinking strengthening mechanisms to achieve hydrogels with stronger mechanical properties better suited for applications in soft robotics (>1 MPa). Chapter 4 summarizes the work and provides an outlook on future research.

1.4 References

[1] Liu, K.; Wei, S.; Song, L.; Liu, H.; Wang, T.; Conductive Hydrogels—A Novel material: Recent Advances and Future Perspectives. *Journal of Agricultural and Food Chemistry* **2020,** *68*, 7269-7280. https://doi.org/10.1021/acs.jafc.0c00642

[2] Ahmed, E. M. Hydrogel: Preparation, characterization, and applications: A review. *J. Adv. Res.* **2015**, *6*, 105– 121. https://doi.org/10.1016/j.jare.2013.07.006

[3] Peng, Q.; Chen, J.; Wang, T.; Peng, X.; Liu, J.; Wang, X.; Wang, J.; Zeng, H. Recent advances in designing conductive hydrogels for flexible electronics. *InfoMat*. **2020**, *2*, 843– 865. https://doi.org/10.1002/inf2.12113

[4] Chen, Y.; Kim, Y.-S.; Tillman, B.W.; Yeo, W.-H.; Chun, Y. Advances in Materials for Recent Low-Profile Implantable Bioelectronics. *Materials* **2018**, *11*, 522. https://doi.org/10.3390/ma11040522

[5] Ashby, M.F. Materials selection strategies. In *Materials and the Environment,* 2nd ed.; Butterworth-Heinemann, 2013; pp 227-273. https://doi.org/10.1016/B978-0-12-385971-6.00009-9

[6] Akhtar, R.; Sherratt, M.J.; Cruickshank, J. K.; Derby, B. Characterizing the elastic properties of tissues. *Materials Today* **2011**, *14*, 96-105. https://doi.org/10.1016/S1369-7021(11)70059-1

[7] Silver, F.H.; Bradica, G.; Tria, A. Elastic energy storage in human articular cartilage: estimation of the elastic modulus for type II collagen and changes associated with osteoarthritis. *Matrix Biology* **2002**, *21*, 129-137. https://doi.org/10.1016/S0945-053X(01)00195-0

[8] Ji, D; Kim, J. Recent Strategies for Strengthening and Stiffening Tough Hydrogels. *Adv. NanoBiomed Res.* **2021,** *1*, 2100026. https://doi.org/10.1002/anbr.202100026

[9] Kayser, L. v.; Lipomi, D. J. Stretchable Conductive Polymers and Composites Based on PEDOT and PEDOT:PSS. *Advanced Materials* **2019**, *31*, 1–13. https://doi.org/10.1002/adma.201806133.

[10] Zhou, T.; Gao, X.; Dong, B.; Sun, N.; Zheng, L. Poly(ionic liquid) hydrogels exhibiting superior mechanical and electrochemical properties as flexible electrolytes. *J. Mater. Chem. A* **2016**, *4*, 1112-1118. https://doi.org/10.1039/C5TA08166A

[11] Wang, Y.; Zhu, C.; Pfattner, R.; Yan, H.; Jin, L.; Chen, S.; Molina-Lopez, F.; Lissel, F.; Liu, J.; Rabiah, N. I.; Chen, Z.; Chung, J. W.; Linder, C.; Toney, M. F.; Murmann, B.; Bao, Z. A Highly Stretchable, Transparent, and Conductive Polymer. *Science Advances* **2017**, *3*, 1-11. https://doi.org/10.1126/sciadv.1602076.

[12] Liu, Y.; Liu, J.; Chen, S.; Lei, T.; Kim, Y.; Niu, S.; Wang, H.; Wang, X.; Foudeh, A.M.; Tok, J.B.-H.; Bao, Z. Soft and elastic hydrogel-based microelectronics for localized low-voltage neuromodulation. *Nat. Biomed. Eng.* **2019,** *3*, 58–68. https://doi.org/10.1038/s41551-018-0335-6

Chapter 2: Mechanically tunable and conductive hydrogels compatible via DLP 3D printing

2.1 Introduction

Electronics that have mechanical properties easily tunable to those of biological tissues are required to realize a seamless integration with biological systems. Materials that can achieve electrical conductivity, conformal contact, and a certain degree of stretchability to keep up with dynamic tissue surfaces are required to achieve this. Biological tissues can range from 0.5-1 kPa[1] for soft tissues such as the brain to about 50-100 kPa[2] for tissues such as breast tissue or epidermal skin. Because of this requirement, traditionally conductive materials such as noble metals are ill-suited to these applications due to their limited stretchability[3, 4]. Conducting polymer hydrogels haver emerged as a good way to obtain conductivity and biologically relevant mechanical properties in the same material. Particularly, 3D printability of the conductive material is also a desirable trait as this enables rapid patterning and realization of complex structures, expanding the materials potential to the realm of bioelectronics [6], actuation [7] and wearable applications [8]. By blending in photopolymerizable hydrogels, the conducting polymer and hydrogel blend can potentially achieve a compromise between good conductivity, soft mechanical properties, and 3D printability.

Typical conductive polymers used for these purposes include polyaniline (PANI) [9], Polypyrrole (PPy) [10] and poly(3,4-ethylenedioxythiophene) polystyrene sulfonate (PEDOT:PSS) [11]. PEDOT:PSS is one of the most successfully used conductive polymers in literature, having a high reported conductivity and easy solution processability [12]. Unlike other conductive polymers, PEDOT:PSS exhibits excellent biocompatibility as well as high conductivity [3]. In addition to these properties, achieving a one-pot preparation with PEDOT:PSS hydrogel is

highly desirable as it is a gateway to achieving high resolution and complex structures via additive manufacturing techniques such as 3D printing which can lead to innovations in areas such as soft robotics [13], biomedical devices [14], and wearable sensors [15]. There are a couple of ways to realize the 3D printing of PEDOT:PSS-based conductive hydrogels. Pure PEDOT:PSS hydrogels can be achieved by solvent casting and annealing a PEDOT:PSS solution into a thin film configuration and then rehydrating them to obtain a hydrogel [11, 20]. While this method can achieve extremely high conductivities (20-40 S/cm), it leads to low stretchability (20-35%) and a modulus (1-2 MPa) that is still orders of magnitude larger than that exhibited by biological tissues, not to mention a long fabrication time. Other methods such as the addition of high concentrations of freeze-dried PEDOT:PSS [23] may increase the conductivity and still be printable but fall short in terms of mechanical properties. A new method that has emerged to increase conductivity and maintain mechanical properties in solution based PEDOT:PSS is the addition of ionic liquids such as 4-(3-Butyl-1-imidazolio)-1-butanesulfonic acid triflate as they have demonstrated they can induce high conductivity in PEDOT:PSS hydrogels [17]. The ionic liquid can both dope the conjugated polymer chains as well as weaken the interactions between the hard conductive PEDOT domains and the soft, insulating PSS chains enabling the PEDOT domains to have easier access to each other and therefore increasing the materials conductivity[18]. However, ionic liquid has never been used to obtain a 3D printable conductive hydrogel. It is therefore still challenging to obtain a conductive hydrogel capable of compromising between good conductivity, stretchability, and the ability to be 3D printed.

Here, we systematically studied the compatibility and interaction of a conducting polymer, with common polymers used for hydrogel 3D preparation, and present a one-pot UV-curable conductive hydrogel with solution based, low concentration PEDOT:PSS, ionic liquid, and

acrylamide. The combination of the acrylamide and the ionic liquid is the key aspect that enables the novel properties presented in this work.Acrylamide (AAm) is capable of pre-initiating the conformational change of PEDOT:PSS due to its strong hydrogen bonding capabilities with PSS, and with the addition of ionic liquid, the conductivity is increased as the electrostatic interactions between PEDOT and PSS are weakened, freeing up the PEDOT domains to aggregate and form conductive pathways. Moreover, the innate stretchability of polyacrylamide (PAAm) allows for the biologically relevant mechanical properties that are desired and the incorporation of ionic liquid does not significantly compromise this aspect. Finally, the addition of a photoinitiator allowed for UV-crosslinking of the conducting hydrogels via a digital light processing (DLP) 3D printing technique. Complex patterns can be obtained in a few seconds, and no other post-processing is needed to obtain a printable, conductive, and stretchable hydrogel. The resulting material leverages the mechanical properties of the PAAm hydrogel, and the electrical conductivity benefits the combination of PAAm and the ionic liquid affords the PEDOT:PSS, resulting in a hydrogel that is highly conductive (2.61-18.49 S/m), stretchable (250-810%) and capable of demonstrating tissue like mechanical properties (7.05-96.30 kPa). This approach enabled the quick construction of complex 2D shapes and 3D overhanging structures without the use of any molds, as well as a strain sensor capable of monitoring a wide range of human motions. The intersection of good conductivity, stretchability, and 3D printability showcases this works advantages and promise in the fabrication and development of electronics with mechanical properties in biologically relevant ranges.

2.2 Materials and Methods

Materials

The conductive polymer PEDOT:PSS Clevios™ PH 1000 was acquired from Heraeus with a 1-1.3 wt% PEDOT:PSS solid content. The hydrogel monomers Acrylamide (AAm) and the crosslinking agent N,N'-Methylenebisacrylamide (BIS) were acquired from Fisher Scientific International, Inc. Lithium phenyl-2,4,6-trimethylbenzoylphosphinate (TPO-Li) was utilized as a photoinitiator for the UV-sensitive components and was acquired from CPS Polymers. The ionic liquid used to dope the PEDOT:PSS in this work was 4-(3-Butyl-1-imidazolio)-1-butanesulfonic acid triflate and it was acquired from Santa Cruz Biotechnology. All chemicals were utilized as received. This work did not generate new or unique reagents.

Fabrication UV-curable of PEDOT:PSS/PAAm/Ionic Liquid hydrogel

The UV-curable conductive hydrogel ink was prepared by taking the PEDOT:PSS solution and filtering it with a 0.45μm filter and then vigorously vortexing it before use. The hydrogel monomer was then added in as a weight percentage with respect to the volume of PEDOT:PSS (20% w/v, 30% w/v, 40% w/v, 50% w/v) and stirred vigorously until a uniform solution was obtained. Next, N,N'-Methylenebisacrylamide (BIS) was added to the solution with respect to the weight of the monomer as a crosslinking agent (1% w/w, 1.5% w/w, 2% w/w). TPO-Li constituted the photoinitiator in the ink and was added at a 0.5% (w/v) with respect to the volume of PEDOT:PSS for all samples. The ionic liquid, 4-(3-Butyl-1-imidazolio)-1-butanesulfonic acid triflate, was added into the PAAm/PEDOT:PSS mixture for a final concentration of 2% (w/v) with respect to the PEDOT:PSS solution. Once all if the components where thoroughly mixed, the mixture was centrifuged to remove any bubbles and the ink was ready poured into a glass slide

mold with a 1 mm thickness and exposed to UV light for 300 seconds to ensure complete crosslinking. DI water was used to wash of any unreacted components.

DLP Printing and device fabrication

A home-made direct light processing was utilized to obtain complex 2D patterns and 3D structures. The system consisted of three major components: a UV light projector from Wintech Digital System Technology Corporation (PRO4500) projecting 365 nm light, a motorized stage capable of translational movement to hold the conductive hydrogel ink bath, and optical accessories from Thorlabs, Inc. such as a converging lens and a reflective mirror to focus and align the projected light pattern. Printing was conducted under ambient conditions. A silanized glass slide was used as a printing substrate to ensure adhesion of the first printing layer. Light patterns could be generated either via Microsoft Power Point for 2D patterns or via Autodesk Fusion 360 to obtain 3D patterns and sliced into 2D patterns via the Creation Workshop software. For the overhanging structure, the layer thickness was set to 0.1 mm. Each layer was cured for 10 seconds, and DI water was used to wash of any excess and unreacted ink.

Mechanical and electrical testing

To determine the conductive hydrogels electrical properties a hydrogel sample of 30 mm length, 5 mm width and 1 mm thickness was cut out and placed on a four-electrode array. Based on the obtained resistance and the known dimensions conductivity was calculated via the equation:

$$\sigma = \frac{l}{RA}$$

where l is the length of the hydrogel, A is its cross-sectional area (width times thickness) and R is the resistance measured. Mechanical testing was done using a Cellscale Unistretch tensile tester

with an 8.9N load. By adding carbon cloth to the tensile tester grips as a charge collector both stress and resistance measurements were obtained as a function of the strain placed on the material by connecting the carbon cloth to a Keithley 2450.

Chemical and Microstructure characterization

The conductive hydrogel was immersed into liquid nitrogen after being UV-crosslinked and cut immediately after to expose the inside structure. The sample was then freeze-dried for two days using a Labconco FreeZone freeze-dryer. The vibrational modes of the different freeze-dried hydrogel samples were investigated using a Renishaw inVia confocal Raman microscope system with a 633 nm laser at 50% power in the range from 400-3200 cm^{-1} and after three accumulations. Fourier-transform infrared spectroscopy (FTIR) was applied with an Agilent Technologies Cary 600 Series FTIR spectrometer by embedding about 2% (w/w) of the desired sample into a potassium bromide (KBr) pellet. Measurements were recorded in a 400-4000 cm^{-1} spectral range. To observe the microstructure of the obtained conductive hydrogels, gold was sputtered on to an exposed freeze-dried hydrogels to image the microstructure using a ZEISS Supra 40VP SEM.

Human body motion sensing

Devices for human body motion sensing where fabricated by printing a long strip of the conductive hydrogel and encapsulating the material in Very High Bond 4905 (VHB) 3M tape. Carbon cloth was used as a charge collector. We rationally picked the data starting from device stabilization (around third cycle).

FRESH Support Bath Preparation and Printing

FRESH v2.0 was prepared as described in Lee, et al. [36]. In brief, a 50% (v/v) ethanol solution was placed in a 1L beaker and heated to 45°C. Once this temperature was reached 2.0% (w/v) gelatin Type B, 0.25% (w/v) Pluronic F-127 and 0.1% (w/v) gum arabic were added into the solution and stirred vigorously. Once they completely dissolved an overhead stirrer was employed to form the gelatin microparticles. Stirring was allowed to occur overnight, with the beaker covered in parafilm to minimize evaporation, while the mixture cooled to room temperature. Once removed from the stirrer the resulting material was divided into 50 mL falcon tubes and centrifuged for 10 minutes at 300g to separate the gelatin support bath from the ethanol solution. After the supernatant was discarded, the mixture was resuspended in water and washed three more times in water at 1000g for 2 minutes each wash to remove any excess reactants. The support bath was stored at 4°C until needed for printing. To prepare it for printing, the mixture was centrifuged at 1000g for 10 minutes and then transferred to the appropriate glass containers for printing. All the printing was performed on a Cellink BioX™ 3D printer using the pneumatic printhead. For multi-material printing, a second pneumatic printhead was added to the array. The STL models to be printed were first designed the Autodesk Fusion 360 ™ software and then exported in to the Cellink Heartware software to obtain and edit the G-code commands that the BioX used to print. The prepared FRESH v2 support bath was placed in a glass petri dish or on a glass slide depending on the size and complexity of the print. After the nozzle was aligned and the ink printed the support bath was exposed to UV light. After the ink was cured the print was placed gently into warm water to melt away the support bath.

Dual Material Device Testing: Strain Sensors.

Once the strain sensors were removed from the melted support bath, they were dried by carefully blotting them with Kim wipes and placed on the subject's hand. Copper wires were used to connect the conductive hydrogel ink tracks to a Keithley multimeter to record the resistance changes as a function of the subjects' movements.

Dual Material Device Testing: Light Actuator.

Once the pillar was removed from the melted support bath, it was dried by carefully blotting it with Kim wipes and placed on a glass slide. A laser was pointed towards the spot on the pillar containing the conductive hydrogel ink and turned on for approximately a minute and thirty seconds' while the pillar collapsed towards the light.

2.3 Results and Discussion

As mentioned above, blending in other hydrogel precursors is necessary to reach good mechanical properties. However, not all photopolymerizable hydrogels can easily blend with PEDOT:PSS. We found that polymers with a methacrylate component such as polyvinyl alcohol methacrylate (PVA-MA) and gelatin methacrylate (GelMA) could not mix into PEDOT:PSS at room temperature (Figure 2.1). Direct blending of polyacrylic acid (PAAc) was not possible as the acidity of the monomer caused it to crash out of the PEDOT:PSS solution and resulted in an inhomogeneous mix. Polyacrylamide (PAAm) can easily mix into PEDOT:PSS at room temperature and was therefore selected for this work (Figure 2.1).

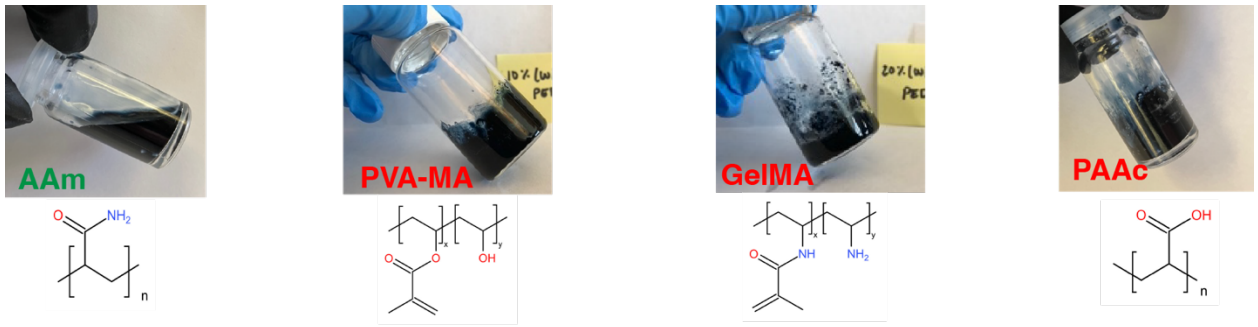

Figure 2.1. Addition of different common polymers to pristine, solution based PEDOT:PSS showing that only PAAm is miscible in the solution at room temperature.

The effect of PEDOT:PSS concentration and physical state (solution-based or freeze-dryed) was then studied. While using commercially available low-concentrated PEDOT:PSS pristine solution (~1 wt%) allows for the selective tuning of the resulting materials mechanical properties based on the properties of the selected hydrogel matrix [21, 22] as well as demonstrated printability, it results in low conductivity (<2 S/m) which is not desirable in most applications. Using lyophilized PEDOT:PSS to increase the PEDOT:PSS solid content can potentially increase the conductivity [23] but it often results in diminished mechanical properties. This was confirmed by mixing freeze-dried PEDOT:PSS into a 20% (w/v) PAAm hydrogel solution. Comparing the pristine, solution based PEDOT:PSS to a similar PEDOT:PSS solid weight percentage in a freeze-dried configuration showed an increase in conductivity from 0.47 S/m to 2.77 S/m (Figure 2.2A). Increasing the freeze-dried solid PEDOT: PSS content to 2% can slightly increase the conductivity to 3.09 S/m. While the conductivity is in the desired range, the mechanical properties of the freeze-dried composites are less than ideal (Figure 2.2B) with a very limited stretchability (<150%) compared to the solution based PEDOT:PSS (> 800%). This factor indicates the need to find another way to increase the conductivity of PEDOT:PSS that does not interfere with the stretchability provided by the PAAm hydrogel matrix.

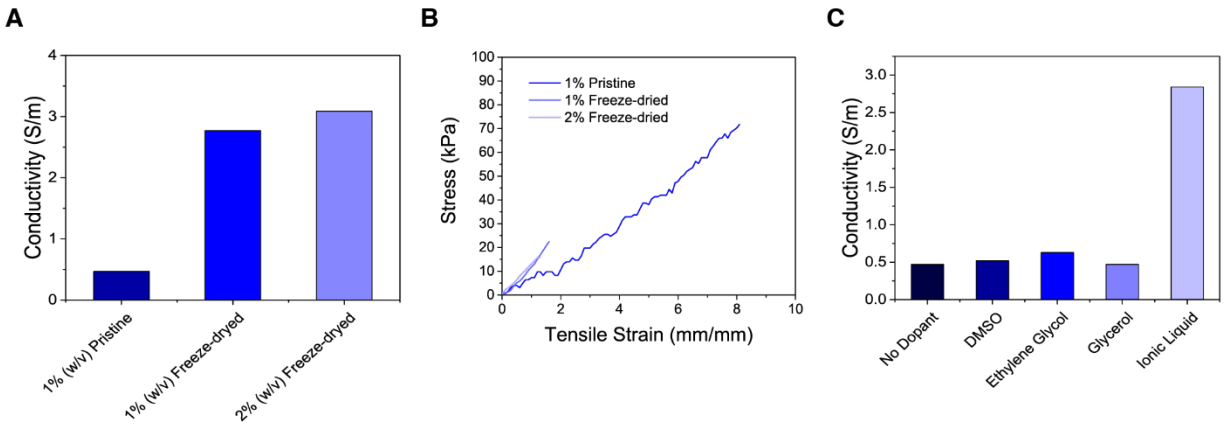

Figure 2.2 (A) Conductivity comparison between pristine, solution based PEDOT:PSS which contains ~1 wt% solid content of PEDOT:PSS and two different wt% solid contents of freeze-dried PEDOT:PSS; all are mixed into a PAAm hydrogel matrix. (B) Stress-strain curve comparison between pristine, solution-based PEDOT:PSS which contains ~1 wt% solid content of PEDOT:PSS and two different wt% solid contents of freeze-dried PEDOT:PSS; all are mixed into a PAAm hydrogel matrix. (C) Conductivity comparison using pristine, solution based PEDOT:PSS mixed into a PAAm hydrogel matrix and doped with different chemical species.

Table 2.1 Properties of tested hydrogel matrices for direct blending with PEDOT:PSS

Hydrogel backbones	Photo-crosslinking	Solubility in Water/PEDOT:PSS	Stretchability
AAm	Yes	Yes	Yes
PVA-MA	Yes	No	NA
GelMA	Yes	No	NA
AAc	Yes	No	NA

To improve the conductivity of the PEDOT:PSS within the PAAm matrix, the incorporation of different dopants was explored. The addition of organic polar solvents such as dimethyl sulfoxide (DMSO)[11, 20], glycerol [24-25], and ethylene glycol [26-27] have been shown to improve the conductivity of PEDOT:PSS both in thin films and in hydrogels. Their presence induces a phase separation of the PEDOT and PSS chains, converting the core PEDOT from a coiled structure to more linearly oriented chains which increase π-π stacking and consequently increases conductivity [26]. While we were able to confirm that the direct addition of these high boiling point solvents does increase the conductivity compared to undoped pristine PEDOT:PSS in a PAAm matrix (Figure 2.2C), the increase in conductivity was relatively minimal. Ionic liquids have recently emerged as a new way to increase the conductivity of PEDOT:PSS by disrupting the electrostatic bonds between the soft insulating PSS chains and the hard conductive PE-DOT domains [17, 18].

Table 2.2 Comparison between the ionic liquid doped conductive hydrogel ink and other 2D patternable/3D printable conductive hydrogel ink in the literature

Hydrogel composition	Conductive Filler and Additives	Printing & Crosslinking method	2D Patterns/ 3D structures	Electrical Properties	Mechanical Properties	Reference
PEDOT:PSS	Pristine PEDOT:PSS/ Ionic liquid	Inkjet printing	Only 2D (300 μm)	σ: 9 x 10^4 S/m	NA	42
PEGDA/ PEDOT:PSS	7 wt% lyophilized PEDOT:PSS/ DMSO	SLA. Photocrosslinking	Only 2D (~385 μm)	R_s: 0.7 to 2.8 kΩ/sq	Modulus: 26.3 to 35.4 MPa	23

					Strain: 60% to 100%	
P(HEMA-co-EGMA)/ PEDOT:PSS	0.0-1.0 wt% Lyophilized PEDOT:PSS/ Rheological modifiers	SLA. UV curing	Both (~450 µm)	R:100 to 125 kΩ	Modulus: 82 kPa Strain: NA	43
PEDOT:PSS	1-10 wt% lyophilized PEDOT:PSS/ DMSO	DIW. Annealing and re-hydrating	Both (~100 µm)	σ: 28 S/cm	Modulus: 1.1 MPa Strain: 20%	20
MC/ kCA/ PEDOT:PSS	0.1-0.3 wt% pristine PEDOT:PSS/ No additives	DIW. Immersion in 5 wt% KCl solution	Both (~100 µm)	σ: 0.3 S/m	Modulus: 8 kPa to 28.5 kPa Strain: 20% to 40%	44
GelMA/ PEDOT:PSS	0.3 wt% pristine PEDOT:PSS/ No additives	FRESH. Support bath with $CaCl_2$, photo-crosslinking, isotherm	Both (~120 µm)	R_s: 261.0 to 281.2 kΩ	Modulus: 40.9kPa to 141.7 kPa Strain: NA	22
PVA-Ph/ EDOT	EDOT 93 mM/ *p*-glycol	DIW. Visible Light	Both (~100 µm)	σ: 0.9 to 2 S/m	Modulus: 800 kPa Strain: 600%	28
PAAm/ PEDOT:PSS	1 wt% pristine PEDOT: PSS/ Ionic Liquid	DLP. UV curing	Both (~150 µm)	σ: 2.61 to 18.49 S/m	Modulus: 7-97 kPa Strain: 250-800%	This work

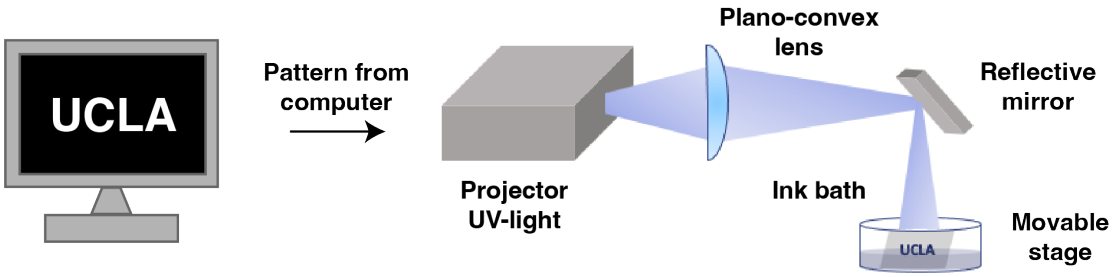

Figure 2.3 Fabrication and patterning process of the one-pot conductive hydrogel ink. A projector capable of outputting UV light is used to project a "UCLA" pattern through a digital mask and on to the conductive hydrogel ink bath.

Once decoupled, the PEDOT can aggregate more effectively, leading to increased conductivity. In addition to this effect, the ionic liquid we selected, 4-(3-Butyl-1-imidazolio)-1-butanesulfonic acid triflate, contains acidic anions that are also capable of doping conducting polymers. The combination of these two mechanisms leads to an increase in conductivity to 2.84 S/m in the presence of ionic liquid (Figure 2.2C). This conductivity is well above the desired range (>2 S/m) as it surpasses the conductivity of the only other identified stretchable and conductive PEDOT:PSS hydrogel capable of producing 3D structures found in literature [28] (Table 2.2) and was therefore selected for further characterization. The use of PAAm in the presence of a photoinitiator such as lithium phenyl-2,4,6-trimethylbenzoylphosphinate (Li-TPO), which is both water-soluble and PEDOT:PSS-soluble, allows for polymerization under a wide range of light spectra, particularly UV-light. N,N'-Methylenebisacrylamide (BIS) is also added to the blend serving as a crosslinking agent. This mixture resulted in a one-pot, conductive and printable hydrogel ink. Using a digital mask, a projector capable of projecting UV light was utilized to project the desired pattern. Using a plano-convex lens and a reflective mirror, the image was maneuvered on to a movable stage containing an ink bath with the ink proposed in this work

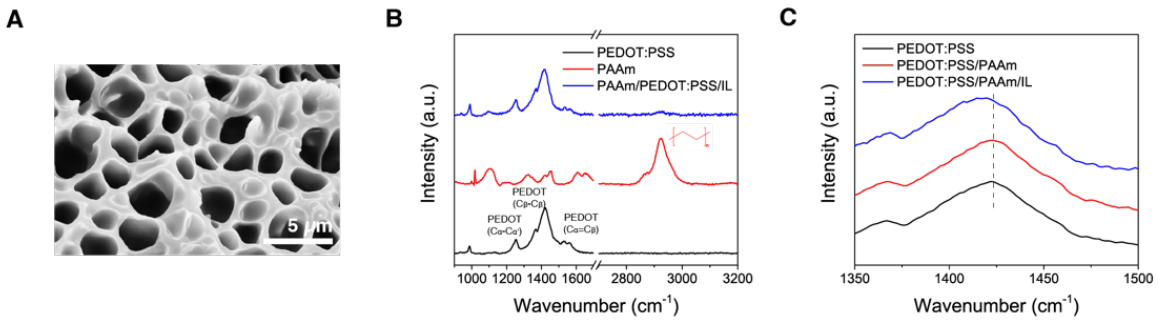

Figure 2.4 (A) Scanning electron microscopy image of the PAAm/PEDOT:PSS/IL hydrogel. (B) Raman spectra of freeze dryed pure PEDOT:PSS, pure PAAm, PAAm/PEDOT:PSS/ IL. (C) Raman spectra of relevant wavenumber ranges for PEDOT:PSS, PAAm/PEDOT:PSS, and PAAm/PEDOT:PSS/ IL.

(Figure 2.3). Using this set-up various complex pattern could be successfully printed which will be showcased later in this work. Due to these favorable properties, this material system was selected for further study and optimization.

Chemical characterization was conducted on the material to better understand its morphology and confirm its composition. A stable porous network is observed via scanning electron microscope (Figure 2.4A), with 2.5 µm sized pores, indicating the uniform distribution of all the components in the PEDOT:PSS/PAAm hydrogel ink doped with ionic liquid. The chemical structures changes after the combination with PAAm and IL treatment were also studied via Raman spectroscopy. A pure PEDOT:PSS sample yielded vibrational mode peaks at 1524 cm^{-1}, 1423 cm^{-1}, 1367 cm^{-1} and 1253 cm^{-1} corresponding to PEDOT C_α=C_β asymmetrical, PEDOT C_α=C_β symmetrical, C_β—C_β stretching mode and the C_α—$C_{\alpha'}$ interring stretching vibrations respectively. The vibrational mode for PSS in the pure PEDOT: PSS sample can be found at 1562 cm^{-1}. The deformation of oxyethylene rings could be observed at the 987 cm^{-1} vibrational mode. For pure polyacrylamide the major Raman band can be found at the 2926 cm^{-1} vibrational mode (Figure 2.4B). The conductive hydrogel ink with a polyacrylamide hydrogel matrix and PEDOT:

PSS as the conductive filler (Figure 2.4B) exhibited a peak shift for the C_α=C_β symmetrical of PEDOT from 1423 cm^{-1} to 1421 cm^{-1}. A shift in the symmetrical C_α=C_β vibrational mode indicates that the structure of the PEDOT domain has changed from a benzoid to a quinoid structure. This change indicates a strong screening effect between the PEDOT and PSS domains and an unraveling from the coiled conformation PEDOT, favored by a benzoid structure, into a more linear configuration, favored by the quinoid structure, occurs [29, 30].

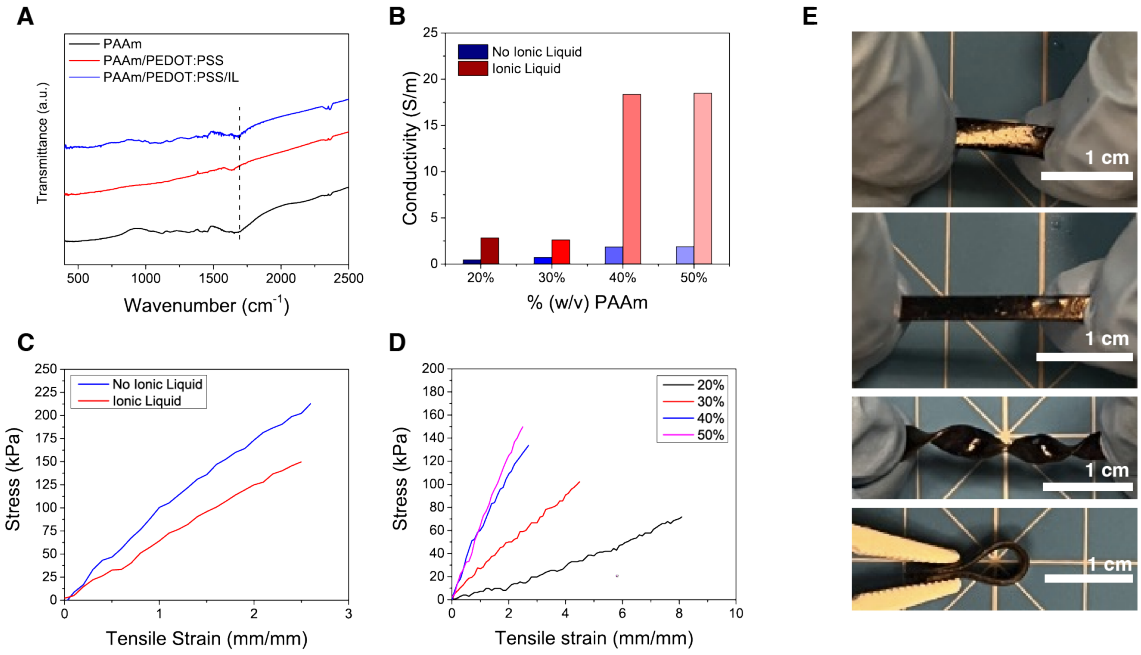

Figure 2.5 (A) FTIR Spectra of pure PAAm, PAAm/PEDOT:PSS and PAAm/PEDOT:PSS/ IL. (B) Conductivity comparison of different PAAm weight percentages both with and without ionic liquid. (C) Stress-strain curve comparison of two different PAAm weight percentages both with and without ionic liquid. (D) Stress-strain curve comparison of different PAAm weight percentages with ionic liquid. (E) Photographs of a 50% (w/v) PAAm/PEDOT:PSS/Ionic liquid sample being stretched, twisted, and bent.

When ionic liquid is added into a PAAm and PEDOT:PSS mixture the redshift becomes more pronounced going to 1419 cm^{-1} (Figure 2.4C). These shifts confirm the role of ionic liquid in enhancing the conductivity of the composite as a more linear configuration of PEDOT allows for

these domains to have easier access to each other and aggregate into longer conductive pathways within the conductive hydrogel. Of note is that even without ionic liquid, PAAm can induce a slight redshift of its own compared to a pure PEDOT:PSS hydrogel sample under Raman spectroscopy. This suggests that PAAm also has a hand in bringing about a beneficial configurational change. Tseng, *et al.* suggests that the addition of soft polymers to PEDOT:PSS can influence the conductivity of the resulting composite as hydrogen bonds are formed between the soft polymers and the soft PSS component. This causes the PSS to pull away slightly from the PEDOT domain allowing for them to start adopting a linear configuration [31]. This was confirmed in this work by measuring the Fourier-transform infrared spectroscopy (FTIR) spectra of the materials (Figure 2.5A). Pure PAAm hydrogel spectra exhibit a peak at around 1660 cm^{-1} corresponding to the C=O stretching, C=C and the C-O-C groups [32]. A peak shift occurs after the addition of PEDOT:PSS to around 1640 cm^{-1} further confirming the interactions between PEDOT:PSS and PAAm. Based on these observations the mechanism this work suggests is as follows: pristine PEDOT:PSS exists in small globules in solution (Figure 2.6A) with the hard PEDOT domains being encased within the soft PSS domains due to the strong electrostatic interactions between them [26]. The addition of AAm pre-initiates a configurational change, with the AAm forming hydrogen bonds with the PSS domain and starting to slightly pull the PSS from the PEDOT as it preferentially bonds with AAm (Figure 2.6B). The addition of ionic liquid complements the disruption the AAm initiated by weaking the interactions between the PEDOT and PSS domains themselves, resulting in a semi-linear configuration where the PEDOT domains have easier access to each other and aggregate into closer conductive pathways (Figure 2.6C). Once the TPO-Li was added, UV light was employed to initiate the crosslinking of AAm around the configurationally changed PEDOT:PSS (Figure 2.6D) and resulted in a conductive hydrogel.

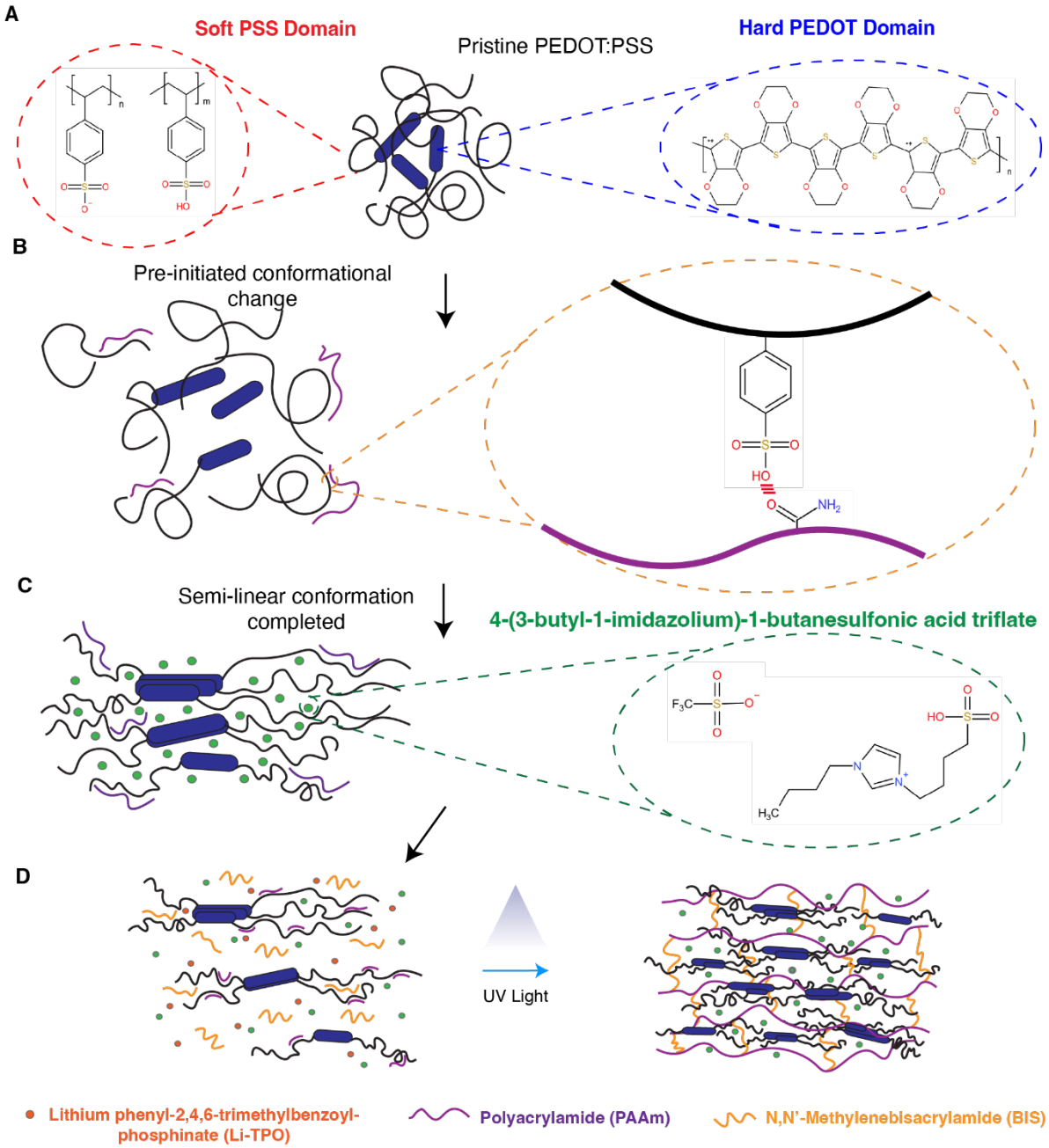

Figure 2.6 Conductivity enhancement mechanism and structure of the one-pot, conductive and printable hydrogel ink. (A) Morphology and structure of pristine PEDOT:PSS. (B) Addition of AAm to PEDOT:PSS initiates a conformational change as the PSS and AAm form hydrogen bonds. (C) Addition of ionic liquid causes a semi-linear conformation as the interactions betweeen PEDOT and PSS are disrupted. (D) After the addition of Li-TPO and BIS, UV light crosslinks the acrylamide monomers around the PEDOT:PSS resulting in a conductive hydrogel.

Table 2.3 Electrical and mechanical characterization of ionic liquid doped conductive hydrogel ink with different hydrogel weight percentages.

AAm %(w/v)	% (w/w) BIS/AAm	Strain at Break (%)	Modulus (kPa)	Conductivity (S/m)
50	2.0	250	96.3	18.49
40	1.0	270	74.61	18.37
30	1.0	450	41.11	2.61
20	0.75	810	7.05	2.84

This mechanism is confirmed with the exhibited electrical properties. Comparing the conductivity of a 20% (w/v) PAAm with PEDOT:PSS to a 50% (w/v) PAAm sample with PEDOT:PSS and no ionic liquid in either sample shows an increase in conductivity from 0.47 S/m to 1.87 S/m (Figure 2.5B). As they contain the same amount of PEDOT:PSS the difference in conductivity can be attributed to the interaction the PAAm has on the PEDOT configuration as confirmed by Raman spectroscopy and FTIR. The addition of ionic liquid further increases the conductivity in both samples; however, the increase depends on the amount of PAAm already in solution, emphasizing the dual pronged approach the hydrogel undergoes with this conductivity enhancement. The inherent mechanical properties the PAAm provides are not significantly affected by the incorporation of the ionic liquid. Experimental results showed that the addition of ionic liquid to a 50% PAAm with PEDOT:PSS sample only affects the mechanical properties slightly (Figure 2.5C). Compared to a sample with the same solid contents with no ionic liquid, the stretchability changes from 260% to 250% and the modulus changes from 103.82 kPa to 96.30

kPa. These changes are minimal and still in the relevant range desired to mimic tissue-relevant mechanical properties. Indeed, a wide assortment of mechanical properties can be obtained by adjusting the PAAm weight percentage in the conductive hydrogel ink (Figure 2.6D) all with conductivities (Figure 3E) well above most printable and stretchable PEDOT:PSS-based conductive hydrogel inks (>2 S/m)(Table 2.3). Even for the stiffest recipe, the conductive hydrogel can be easily stretched, twisted, and bent (Figure 2.5E). All of this suggests a suitability for wearable applications.

Many conductive hydrogels lack the capability to be easily patterned, instead relying on molding to obtain complex patterns and time-consuming crosslinking methods via freeze-drying or heat [33, 17]. Because this work uses a UV-light sensitive hydrogel matrix the resulting conductive hydrogel ink is printable via a direct light processing (DLP). Various complex 2D patterns can be obtained in a matter of seconds such as a grid, a flower, a cartoon dog, and the UCLA cursive logo (Figure 2.7A). The feature sizes that are obtained can be as low as 150 μm. In addition to these 2D patterns, 3D structures can be obtained with overhanging features (Figure 2.7B) by printing multiple layers and be visualized by cutting the grid edge. The resulting prints are proven to still be conductive and capable of powering a red LED (Figure 2.7C) at a constant direct current of 1 mA, which is well below the amount of current the human body can handle without experiencing any muscle disfunction, such as paralysis (>10 mA) [34].

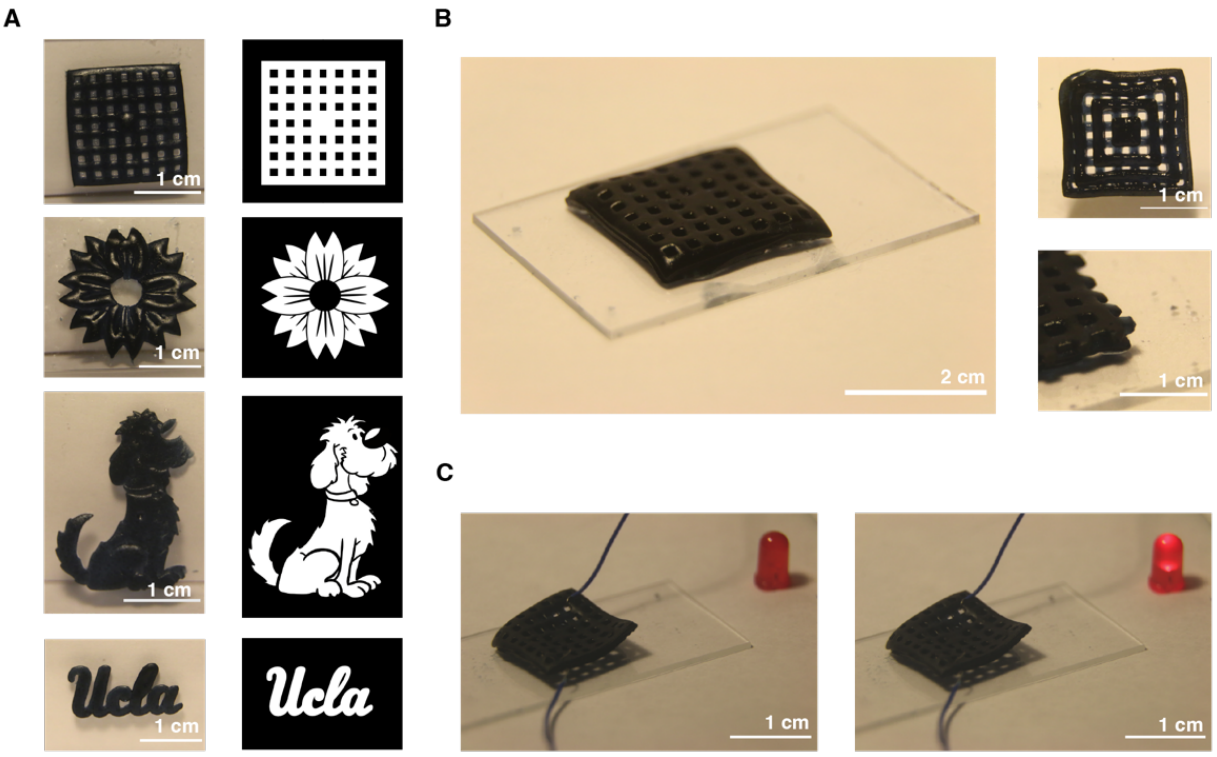

Figure 2.7 Direct light processing (DLP) of conductive hydrogels. A) Printing of different 2D patterns such as a grid, a flower, a cartoon dog, and a UCLA logo on glass. B) Printing of a 3D overhanging structure. C) A DLP printed grid being used to light a red LED.

The printed grid could also be stretched and twisted without any noticeable change in the lighting of the LED. The conductive hydrogel ink was also capable of being printed via a Freeform Reversible Embedding of Suspended Hydrogels (FRESH) approach [35, 36]. This technique is usually implemented to print bio inks which are too low viscosity and therefore not rheologically favorable to be printed via traditional direct ink write (DIW) techniques. Using a gelatin support bath which acts as a Bingham plastic, meaning it holds its shape when at rest and behaves like a liquid at high shear rates, the one pot-conductive hydrogel ink developed in this work can be easily printed in conjunction with other hydrogels to create multi-material devices such as a strain sensor and a light-sensitive collapsible pillar in a very short amount of time (Figure 2.8, 2.9).

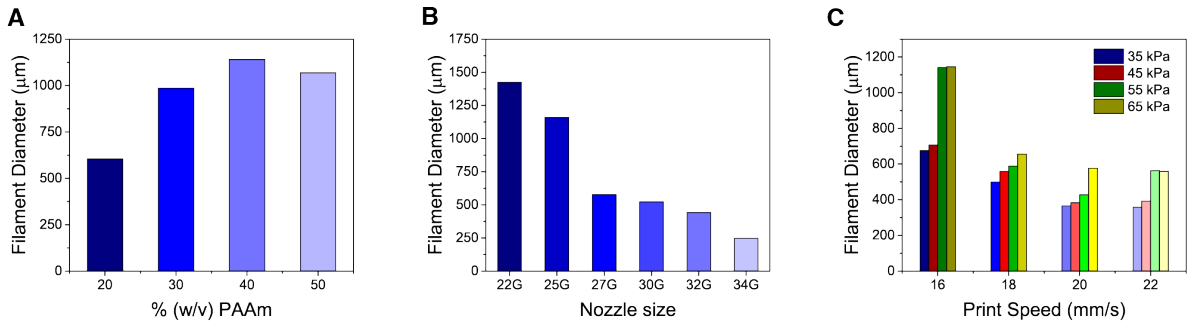

Figure 2.8 Conductive ink hydrogel component optimization for FRESH 3D printing. (A) Filament diameters of ionic liquid doped PEDOT:PSS inks with different PAAm weight percentages. (B) Filament diameter of a 20% PAAm ink with different sized nozzle. (C) Filament diameter of a 20% PAAm ink with a 413 µm sized nozzle at different print speeds and pneumatic pressures.

The developed one-pot synthesis conductive hydrogel, possessing low modulus, high stretchability, and high electrical conductivity, has been demonstrated as a strain sensor capable of detecting both large and subtle human body motions. The ability to monitor and analyze physiological movements has great importance for the correct diagnosis and treatment of patients [37]. Monitoring of movements as subtle as swallowing have been proven useful in the treatment of cancer patients suffering from head and neck post-radiation damage [38]. Devices for monitoring finger movements have also been employed to study patients suffering from carpal tunnel syndrome [39]. Even larger human body motions such as elbow bending have a need to be monitored for subjects recovering from upper limb injuries [40]. In this study, the conductive hydrogel with the highest conductivity and the modulus closest to human skin was utilized as a strain sensor to detect human body motion. After encapsulating the material in a double sided VHB tape to avoid water evaporation and provide adhesion to the skin, the device was placed on

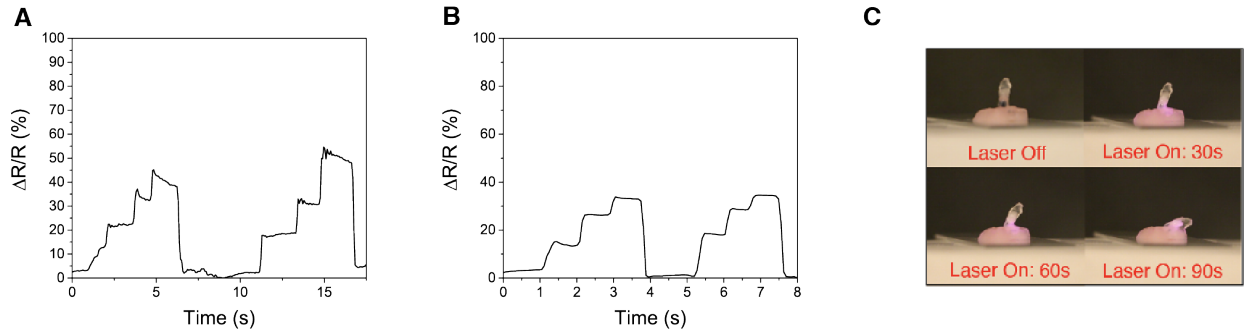

Figure 2.9 Functional multi-material devices via FRESH 3D printing, A) Electrical response of a straight-line strain sensor device to hand bending at different angles, B) Electrical response of a serpentine strain sensor device to finger bending at different angles, B) Electrical response of a serpentine strain sensor device to finger bending at different angles, C) Light sensitive pillar being bent by a laser source over time.

different parts of a human subject's body and the movements recorded. The sensor was able to easily conform to the skin showcasing the materials flexibility and stretchability. The device was clearly capable of detecting small-scale human motions. Swallowing is the process responsible for moving substances from the mouth to the stomach and involves two major mechanical motions.

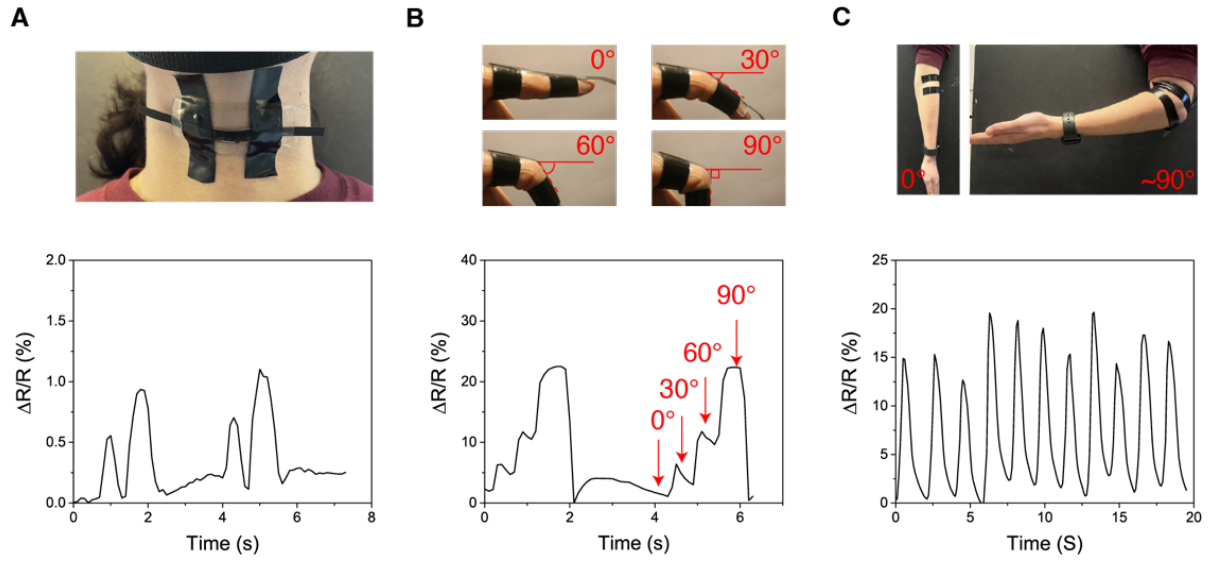

Figure 2.10 Functional wearable strain sensor. Electrical response of the conductive hydrogel to human motion such as A) swallowing, B) finger bending and C) elbow bending.

The first is when the larynx moves upwards and forwards to close the airways and the second is the motion produced by the pharynx as it pushes the bolus, which is whatever small mass of substance is being swallowed such as chewed up food or saliva, down the esophageal [40]. When placed on a subject's throat, the sensor could pick up these two distinct swallowing movements which showcases its promise as a physiological movement sensor (Figure 2.10A). Slightly larger movements such as a finger bending could also be detected by placing the device on the knuckle joint of a finger (Finger 2.10B). The relative change in resistance of the strain sensor clearly exhibited the bending of finger even at different angles and in rapid succession. The response time exhibited by the sensor between each consecutive finger bending was around 0.1 seconds while the response time back from a 90-degree bend to a straight conformation was around 0.2 seconds (Figure 2.11). Additionally, quick, and large deformations could also be detected such as an elbow rapidly bending from a straight arm configuration to about a 90-degree angle (Figure 2.10C). The detection of all these human body motions displays the suitability of this material for applications monitoring both small and larger physiologically relevant deformations.

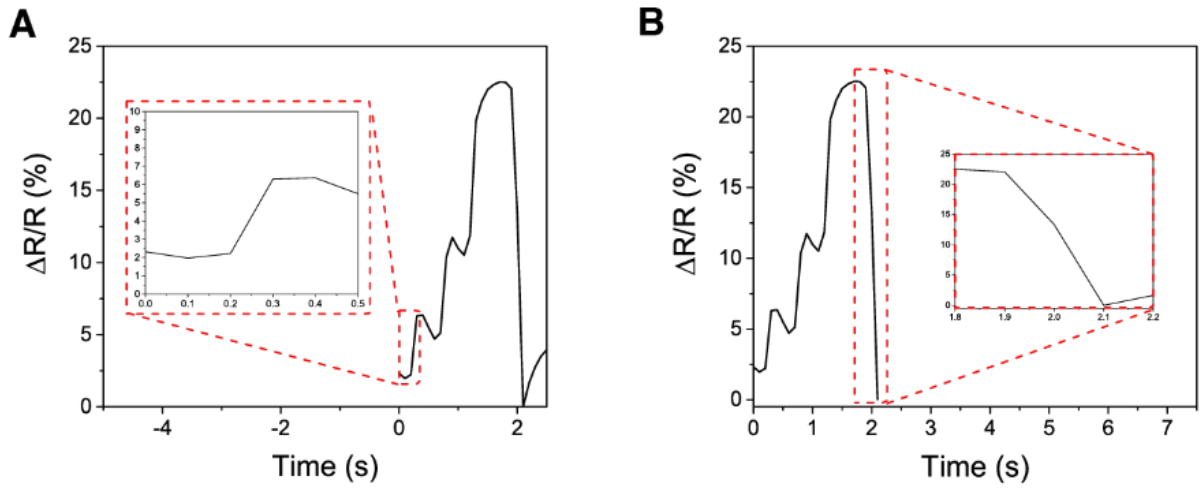

Figure 2.11 Response times for finger bending of strain sensor device fabricated via DLP, (A) at the initial bending to a 30-degree angle and (B) when straightening out after a 90-degree bend.

2.4. Conclusion and Future Work

This work demonstrated a one-pot, UV-crosslinkable, conductive hydrogel with low modulus in tissue relevant ranges and high stretchability. By leveraging the synergic effects that PAAm and ionic liquid have on the morphology and structure of PEDOT:PSS this work was able to obtain a highly conductive hydrogel without sacrificing the inherent mechanical properties that the common polymer hydrogel matrix can offer. In addition to these features, complex patterns and 3D structures were easily obtained via DLP printing after the addition of a photoinitiator. The material was leveraged into human motion body sensing devices showcasing its ability and future in rapid development of flexible and wearable electronics.

3D conductive hydrogels are often used as scaffolds for cell growth. They offer several advantages over traditional two-dimensional cell cultures or even other non-conductive 3D scaffolds. One such advantage is a closer imitation of the actual 3D environment cells experience in the extracellular matrix (ECM), which can have a significant difference in cell behavior such as its proliferation, drug toxicity resistance, gene expression, and differentiation [46]. 3D printing allows for the adjustment of pore size by printing grids with different intra-filament distances (200-2000 μm). This ability has been proven particularly useful in the growth of fibroblasts [47] as these cells are particularly susceptible to this parameter for their viability and proliferation. As this work easily demonstrated grid printing and a resolution as low as 150 μm our material could prove useful in the study of these types of cells.

The ability to be conductive is another major advantage for our printable hydrogel. Electrical stimulation (ES) is a promising biochemical cue used to encourage cell growth. As it imitates a functionality the human body itself already uses, ES is capable of triggering cells to deliver signals via intrinsic pathways that jumpstart the desired cell activities that lead to cell

growth such as migration, differentiation, and proliferation [48]. Biophysical cues such as ES are ideal compared to other forms of stimulating cell growth due to their cost-effectiveness, reproducibility, and potential avenues for large-scale production. ES is preferred over other biochemical cues is due to its ability to relieve pain, reduce vascular and skeletal muscle tension, ability to promote blood circulation as well as its promotion of the re-adsorption of joint fluid in clinical settings [49]. The high conductivity exhibited by our material system should therefore be advantageous to perform ES as a method to improve cell growth. Additionally, hydrogel stiffness (0.1- 100 kPA) has been found to influence how well cells grows on the scaffold [46, 47]. As this work could exhibit a wide range of mechanical properties (modulus 7-97 kPa), it is hypothesized that it would be a good candidate for this type of study.

The one-pot synthesis conductive and printable hydrogel presented in this work should also be well suited as a 3D conductive cell scaffold due to the biocompatibility of all its components. PAAm is a well-established biocompatible polymer that has been used in several 3D cell scaffold studies and has been proven to be growth compatible with many types of cells such as fibroblasts [50], cardiac tissue [51], lung cancer cell [52]. Similarly, PEDOT:PSS is a well-known biocompatible and conductive polymer which has also been previously utilized in the growth of fibroblasts [53], neural cells [23], and bone tissue [54]. While there have been no specific studies done on the cytotoxicity of 4-(3-Butyl-1-imidazolio)-1-butanesulfonic acid triflate, the ionic liquid used in this work, based on its chemical structure similarities with other ionic liquids [55] it can be expected to have low cytotoxicity. 4-(3-Butyl-1-imidazolio)-1-butanesulfonic acid triflate has also been specifically named in a patent filled by Eagle Biologics for a protein subcutaneous or intramuscular injection [56]. They found that at the concentrations they employed, between 20-50 mg/ml, there were no significant signs of toxicity. This works utilizes a concentration of 20 mg/ml

for all the conductive hydrogel inks in addition to employing a washing step after UV-crosslinking to remove excess reactants. This suggests that the inclusion of 4-(3-Butyl-1-imidazolio)-1-butanesulfonic acid triflate in the 3D scaffold would not significantly impact cell growth. Based on all these findings, we believe that the material system developed in this work would be an excellent candidate for electrical stimulation of 3D printed cell-growth scaffolds.

2.6 References

[1] Pettikiriarachchi, J. T. S.; Parish, C. L.; Shoichet, M. S.; Forsythe, J. S.; Nisbet, D. R. Biomaterials for brain tissue engineering. *Aust. J. Chem*. **2010,** *63*, 1143–1154. https://doi.org/10.1071/CH10159

[2] Singh, G.; Chanda, A. Mechanical properties of whole-body soft human tissues: a review. *Biomedical Materials* **2021**, *16*, 062004. https://doi.org/10.1088/1748-605X/ac2b7a

[3] Tang, L.; Wu, S.; Qu, J.; Gong, L.; Tang, J. A Review of Conductive Hydrogel Used in Flexible Strain Sensor. *Materials* **2020**, *13*, 3947. https://doi.org/10.3390/ma13183947

[4] Reichert W.M. *Indwelling Neural Implants: Strategies for Contending with the In Vivo Environment*; Boca Raton (FL): CRC Press/Taylor & Francis, 2008. PMID: 21204399.

[5] Lu, H.; Zhang, N.; Ma, M. Electroconductive Hydrogels for Biomedical Applications. *Wiley Interdisciplinary Reviews: Nanomedicine and Nanobiotechnology* **2019**, *11*, 1–15. https://doi.org/10.1002/wnan.1568

[6] Fu, F.; Wang, J.; Zeng, H.; Yu, J. Functional Conductive Hydrogels for Bioelectronics. *ACS Materials Letters* **2020**, *2*, 1287–1301. https://doi.org/10.1021/acsmaterialslett.0c00309.

[7] Lo, C.-Y.; Zhao, Y.; Kim, C.; Alsaid, Y.; Khodambashi, R.; Peet, M.; Fisher, R.; Marvi, H.; Berman, S.; Aukes, D.; He, X. Highly Stretchable Self-Sensing Actuator Based on Conductive

Photothermally-Responsive Hydrogel. *Materials Today* **2021**, *50*, 35-43. https://doi.org/10.1016/j.mattod.2021.05.008

[8] Chen, Z.; Chen, Y.; Hedenqvist, M. S.; Chen, C.; Cai, C.; Li, H.; Liu, H.; Fu, J. Multifunctional Conductive Hydrogels and Their Applications as Smart Wearable Devices. *Journal of Materials Chemistry B* **2021**, *9*, 2561–2583. https://doi.org/10.1039/d0tb02929g.

[9] Xue, J.; Liu, Y.; Darabi, M. A.; Tu, G.; Huang, L.; Ying, L.; Xiao, B.; Wu, Y.; Xing, M.; Zhang, L.; Zhang, L. An Injectable Conductive Gelatin-PANI Hydrogel System Serves as a Promising Carrier to Deliver BMSCs for Parkinson's Disease Treatment. *Materials Science and Engineering C* **2019**, *100*, 584–597. https://doi.org/10.1016/j.msec.2019.03.024.

[10] Wang, S.; Lei, J.; Yi, X.; Yuan, L.; Ge, L.; Li, D.; Mu, C. Fabrication of Polypyrrole-Grafted Gelatin-Based Hydrogel with Conductive, Self-Healing, and Injectable Properties. *ACS Applied Polymer Materials* **2020**, *2*, 3016–3023. https://doi.org/10.1021/acsapm.0c00468.

[11] Lu, B.; Yuk, H.; Lin, S.; Jian, N.; Qu, K.; Xu, J.; Zhao, X. Pure PEDOT:PSS Hydrogels. *Nature Communications* **2019**, *10*. https://doi.org/10.1038/s41467-019-09003-5.

[12] Fan, X.; Nie, W.; Tsai, H.; Wang, N.; Huang, H.; Cheng, Y.; Wen, R.; Ma, L.; Yan, F.; Xia, Y. PEDOT:PSS for Flexible and Stretchable Electronics: Modifications, Strategies, and Applications. *Advanced Science* **2019**, *6*, 1900813. https://doi.org/10.1002/advs.201900813.

[13] Sun W.; Schaffer, S.; Dai, K.; Yao, .;, Feinberg, A.; Webster-Wood, V. 3D Printing Hydrogel-Based Soft and Biohybrid Actuators: A Mini-Review on Fabrication Techniques, Applications, and Challenges. *Front. Robot. AI*, **2021,** *8*, 673533. https://doi.org/10.3389/frobt.2021.673533

[14] Caló, E.; Khutoryanskiy, V. v. Biomedical Applications of Hydrogels: A Review of Patents and Commercial Products. *European Polymer Journal* **2015**, *65*, 252–267. https://doi.org/10.1016/j.eurpolymj.2014.11.024.

[15] Buenger, D.; Topuz, F.; Groll, J. Hydrogels in Sensing Applications. *Progress in Polymer Science* **2012**, *37*, 1678–1719. https://doi.org/10.1016/j.progpolymsci.2012.09.001.

[16] Subramani, R.; Izquierdo-Alvarez, A.; Bhattacharya, P.; Meerts, M.; Moldenaers, P.; Ramon, H.; van Oosterwyck, H. The Influence of Swelling on Elastic Properties of Polyacrylamide Hydrogels. *Frontiers in Materials* **2020**, *7*, 1–13. https://doi.org/10.3389/fmats.2020.00212.

[17] Feig, V. R.; Tran, H.; Lee, M.; Bao, Z. Mechanically Tunable Conductive Interpenetrating Network Hydrogels That Mimic the Elastic Moduli of Biological Tissue. *Nature Communications* **2018**, *9*, 1–9. https://doi.org/10.1038/s41467-018-05222-4.

[18] Wang, Y.; Zhu, C.; Pfattner, R.; Yan, H.; Jin, L.; Chen, S.; Molina-Lopez, F.; Lissel, F.; Liu, J.; Rabiah, N. I.; Chen, Z.; Chung, J. W.; Linder, C.; Toney, M. F.; Murmann, B.; Bao, Z. A Highly Stretchable, Transparent, and Conductive Polymer. *Science Advances* **2017**, *3*, 1–11. https://doi.org/10.1126/sciadv.1602076.

[19] Wang, Z.; Chen, L.; Chen, Y.; Liu, P.; Duan, H.; Cheng, P. 3D Printed Ultrastretchable, Hyper-Antifreezing Conductive Hydrogel for Sensitive Motion and Electrophysiological Signal Monitoring. *Research* **2020**, *2020*, 1–11. https://doi.org/10.34133/2020/1426078.

[20] Yuk, H.; Lu, B.; Lin, S.; Qu, K.; Xu, J.; Luo, J.; Zhao, X. 3D Printing of Conducting Polymers. *Nature Communications* **2020**, *11*, 1604. https://doi.org/10.1038/s41467-020-15316-7.

[21] Gotovtsev, P. M.; Badranova, G. U.; Zubavichus, Y. V.; Chumakov, N. K.; Antipova, C. G.; Kamyshinsky, R. A.; Presniakov, M. Yu.; Tokaev, K.; Grigoriev, T. E. Electroconductive

PEDOT:PSS-based hydrogel prepared by freezing-thawing method. *Heliyon*, **2019**, *5*, 02498. https://doi.org/10.1016/j.heliyon.2019.e02498

[22] Spencer, A. R.; Shirzaei Sani, E.; Soucy, J. R.; Corbet, C. C.; Primbetova, A.; Koppes, R. A.; Annabi, N. Bioprinting of a Cell-Laden Conductive Hydrogel Composite. *ACS Applied Materials and Interfaces* **2019**, *11*, 30518–30533. https://doi.org/10.1021/acsami.9b07353.

[23] Heo, D. N.; Lee, S. J.; Timsina, R.; Qiu, X.; Castro, N. J.; Zhang, L. G. Development of 3D Printable Conductive Hydrogel with Crystallized PEDOT:PSS for Neural Tissue Engineering. *Materials Science and Engineering C* **2019**, *99*, 582–590. https://doi.org/10.1016/j.msec.2019.02.008.

[24] Zhang, S.; Ling, H.; Chen, Y.; Cui, Q.; Ni, J.; Wang, X.; Hartel, M. C.; Meng, X.; Lee, K.; Lee, J.; Sun, W.; Lin, H.; Emaminejad, S.; Ahadian, S.; Ashammakhi, N.; Dokmeci, M. R.; Khademhosseini, A.; Hydrogel-Enabled Transfer-Printing of Conducting Polymer Films for Soft Organic Bioelectronics. *Adv. Funct. Mater*. **2020**, *30*, 1906016. https://doi.org/10.1002/adfm.201906016

[25] Abd Wahid, N. A.; Hashemi, A.; Evans, J. J.; Alkaisi, M. M; Conductive Bioimprint Using Soft Lithography Technique Based on PEDOT:PSS for Biosensing. *Bioengineering (Basel, Switzerland),* **2021**, *8*, 204. https://doi.org/10.3390/bioengineering8120204

[26] Kayser, L. v.; Lipomi, D. J. Stretchable Conductive Polymers and Composites Based on PEDOT and PEDOT:PSS. *Advanced Materials* **2019**, *31*, 1–13. https://doi.org/10.1002/adma.201806133.

[27] Oh, J. Y.; Kim, S.; Baik, H. K.; Jeong, U. Conducting Polymer Dough for Deformable Electronics. *Advanced materials (Deerfield Beach, Fla.)* **2016**, *28*, 4455–4461. https://doi.org/10.1002/adma.201502947

[28] Wei, H.; Lei, M.; Zhang, P.; Leng, J.; Zheng, Z.; Yu, Y. Orthogonal photochemistry-assisted printing of 3D tough and stretchable conductive hydrogels. *Nat Commun* **2021,** *12*, 2082. https://doi.org/10.1038/s41467-021-21869-y

[29] Yao, B. W.; Wang, H. Y.; Zhou, Q. Q.; Wu, M. M.; Zhang, M.; Li, C.; Shi, G. Q.; *Adv. Mater.* **2017**, *29*, 1700974. https://doi.org/10.1002/adma.201700974

[30] Ouyang, J.; Xu, Q.; Chu, C.-W.; Yang, Y.; Li, G.; Shinar, J. On the mechanism of conductivity enhancement in poly(3,4-ethylenedioxythiophene):poly(styrene sulfonate) film through solvent treatment. *Polymer*, **2004** *45*, 8443–8450. https://doi.org/10.1016/j.polymer.2004.10.001

[31] Tseng, Y.-T.; Lin, Y.-C.; Shih, C.-C.; Hsieh, H.-C.; Lee, W.-Y.; Chiu, Y.-C.; Chen, W.-C. Morphology and properties of PEDOT:PSS/soft polymer blends through hydrogen bonding interaction and their pressure sensor application. *J. Mater. Chem. C*, 2020, *8*, 6013–6024. https://doi.org/10.1039/D0TC00559B

[32] Aouada, F.; de Moura, M.; Radovanovic, E.; Girotto, E.; Rubira, A.; Muniz, E. PAAm and PEDOT/PSS hydrogel as potential electroactive devices: evaluation of surface and hydrophilic properties. *e-Polymers* **2008**, *8,* 154. https://doi.org/10.1515/epoly.2008.8.1.1781

[33] Peng, Y.; Yan, B.; Li, Y.; Lan, J.; Shi, L.; Ran, R. Antifreeze and Moisturizing High Conductivity PEDOT/PVA Hydrogels for Wearable Motion Sensor. *Journal of Materials Science* **2020**, *55*, 1280–1291. https://doi.org/10.1007/s10853-019-04101-7.

[34] Kouwenhoven, W.B.; Effects of electricity on the human body. *Electrical Engineering*, **1949,** *68*, 199-203. doi: 10.1109/EE.1949.6444654

[35] Shiwarski, D. J.; Hudson, A. R.; Tashman, J. W.; Feinberg, A. W. Emergence of FRESH 3D Printing as a Platform for Advanced Tissue Biofabrication. *APL Bioengineering* **2021**, *5*, 010904. https://doi.org/10.1063/5.0032777.

[36] Lee, A.; Hudson, A. R.; Shiwarski, D.J.; Tashman, J. W.; Hinton, T. J.; Yerneni, S.; Bliley, J. M.; Campbell, P. G.; Feinberg, A. W. 3D bioprinting of collagen to rebuild components of the human heart. *Science* **2019**, *365*, 482-487. https://doi.org/10.1126/science.aav9051

[37] Nascimento, L.M.S.D.; Bonfati, L.V.; Freitas, M.B.; Mendes, Junior J.J.A.; Siqueira, H.V.; Stevan, S.L. Sensors and Systems for Physical Rehabilitation and Health Monitoring-A Review. *Sensors (Basel).* **2020**, *20*, 4063. https://doi.org/10.3390/s20154063

[38] Ramírez, J.; Rodriquez, D.; Qiao, F.; Warchall, J.; Rye, J.; Aklile, E.; S-C Chiang; A., Marin, B. C.; Mercier, P. P.; Cheng, C. K.; Hutcheson, K. A.; Shinn, E. H.; Lipomi, D. J. Metallic Nanoislands on Graphene for Monitoring Swallowing Activity in Head and Neck Cancer Patients. *ACS nano* **2018**, *12*, 5913–5922. https://doi.org/10.1021/acsnano.8b02133

[39] Kuroiwa, T.; Nimura, A.; Takahashi, Y.; Sasaki, T.; Koyama, T.; Okawa, A.; Fujita, K. Device Development for Detecting Thumb Opposition Impairment Using Carbon Nanotube-Based Strain Sensors. *Sensors (Basel, Switzerland)* **2020**, *20*, 3998. https://doi.org/10.3390/s20143998

[40] Jakob, I.; Kollreider, A.; Germanotta, M.; Benetti, F.; Cruciani, A.; Padua, L.; Aprile, I. Robotic and Sensor Technology for Upper Limb Rehabilitation. *PM&R* **2018**, *10*, S189-S197. https://doi.org/10.1016/j.pmrj.2018.07.011

[41] Matsuo, K.; Palmer, J. B. Anatomy and physiology of feeding and swallowing: normal and abnormal. *Physical medicine and rehabilitation clinics of North America* **2008**, *19*, 691–vii. https://doi.org/10.1016/j.pmr.2008.06.001

[42] Teo, M. Y.; Ravichandran, N.; Kim, N.; Kee, S.; Stuart, L.; Aw, K. C.; Stringer, J. Direct Patterning of Highly Conductive PEDOT:PSS/Ionic Liquid Hydrogel via Microreactive Inkjet Printing. *ACS Applied Materials and Interfaces* **2019**, *11*, 37069–37076. https://doi.org/10.1021/acsami.9b12069.

[43] Aggas, J. R.; Abasi, S.; Phipps, J. F.; Podstawczyk, D. A.; Guiseppi-Elie, A. Microfabricated and 3-D Printed Electroconductive Hydrogels of PEDOT:PSS and Their Application in Bioelectronics. *Biosensors and Bioelectronics* **2020**, *168*, 112568. https://doi.org/10.1016/j.bios.2020.112568.

[44] Rastin, H.; Zhang, B.; Bi, J.; Hassan, K.; Tung, T. T.; Losic, D. 3D Printing of Cell-Laden Electroconductive Bioinks for Tissue Engineering Applications. *Journal of Materials Chemistry B* **2020**, *8*, 5862–5876. https://doi.org/10.1039/d0tb00627k.

[45] Athukorala, S. S.; Tran, T. S.; Balu, R.; Truong, V. K.; Chapman, J.; Dutta, N. K.; Choudhury, N. R. 3D Printable Electrically Conductive Hydrogel Scaffolds for Biomedical Applications: A Review. *Polymers* **2021**, *13*, 1–21. https://doi.org/10.3390/polym13030474.

[46] Campuzano, S.; Pelling, A. E. Scaffolds for 3D Cell Culture and Cellular Agriculture Applications Derived from Non-animal Sources. *Frontiers in Sustainable Food Systems* **2019,** *3*. https://doi.org/10.3389/fsufs.2019.00038

[47] R. Ibañez, R.I.; do Amaral, R.J.F.C.; Reis, R.L.; Marques, A.P.; Murphy, C.M.; O'Brien, F.J. 3D-Printed Gelatin Methacrylate Scaffolds with Controlled Architecture and Stiffness Modulate the Fibroblast Phenotype towards Dermal Regeneration. *Polymers* **2021**, *13*, 2510. https://doi.org/10.3390/polym13152510

[48] Chen, C., Bai, X., Ding, Y. *et al.* Electrical stimulation as a novel tool for regulating cell behavior in tissue engineering. *Biomater. Res.* **2019**, *23*, 25. https://doi.org/10.1186/s40824-019-0176-8

[49] Hernández-Bule. M.L.; Trillo, M.Á.; Úbeda, A. Molecular Mechanisms Underlying Antiproliferative and Differentiating Responses of Hepatocarcinoma Cells to Subthermal Electric Stimulation. *PLoS ONE* **2014**, *9*. https://doi.org/10.1371/journal.pone.0084636

[50] Solon, J.; Levental, I.; Senguptam K.; Georges, P.C.; Janmey, P.A. Fibroblast Adaptation and Stiffness Matching to Soft Elastic Substrates. *Biophysical Journal* **2007**, *93*, 4453-4461. https://doi.org/10.1529/biophysj.106.101386

[51] Dattola, E.; Parrotta, E. I.; Scalise, S.; Perozziello, G.; Limongi, T.; Candeloro, P.; Coluccio, M. L.; Maletta, C.; Bruno, L.; de Angelis, M. T.; Santamaria, G.; Mollace, V.; Lamanna, E.; di Fabrizio, E.; Cuda, G. Development of 3D PVA scaffolds for cardiac tissue engineering and cell screening applications. *RSC Adv.*, **2019** *9*, 4246–4257. https://doi.org/10.1039/C8RA08187E

[52] Hu, Q.; Liu, X.; Liu, H.; Yang, L.; Yuan, X.; Chen, Y.; Wu, W.; Luo, J.; Long, J.; Huang, M.; Gou, M. 3D printed porous microgel for lung cancer cells culture in vitro. *Materials & Design* **2021,** *210*, 110079. https://doi.org/https://doi.org/10.1016/j.matdes.2021.110079

[53] Zhang, C.; Wang, M.; Jiang, C.; Zhu, P.; Sun, B.; Gao, Q.; Gao, C.; Liu, R. Highly adhesive and self-healing γ-PGA/PEDOT:PSS conductive hydrogels enabled by multiple hydrogen bonding for wearable electronics. *Nano Energy* **2022**, *95*, 106991. https://doi.org/https://doi.org/10.1016/j.nanoen.2022.106991

[54] Guex, A. G.; Puetzer, J. L.; Armgarth, A.; Littmann, E.; Stavrinidou, E.; Giannelis, E. P.; Malliaras, G. G.; Stevens, M. M. Highly porous scaffolds of PEDOT:PSS for bone tissue engineering. *Acta biomater.* **2017**, *62*, 91–101. https://doi.org/10.1016/j.actbio.2017.08.045

[55] Musiał, M.; Zorębski, E.; Malarz, K.; Kuczak, M.; Mrozek-Wilczkiewicz, A.; Jacquemin, J.; Dzida, M. Cytotoxicity of Ionic Liquids on Normal Human Dermal Fibroblasts in the Context of Their Present and Future Applications. *ACS Sustainable Chemistry & Engineering* **2021,** *9*, 7649–7657. https://doi.org/10.1021/acssuschemeng.1c02277

[56] Eagle Biologics, Inc. Liquid protein formulations containing 4-(3-butyl-1-imidazolio)-1-butane sulfonate (BIM). US patent 10,821,183, filed 10 November 2017, issued 3 November 2020.

Chapter 3: UV-patternable, strong, conductive, and stretchable hydrogels

3.1 Introduction

Electrically conductive materials with both a high degree of strength and mechanically compliant properties are widely needed for the development of soft actuators and soft robots. The inclusion of such materials is what allows these types of devices to safely interact with their environment, as rigid components constitute a safety hazard when in proximity with humans, as well as enables the integration of them within biological systems such as in medically needed prosthetics and enhancements designed for locomotor strategies or disaster relief [1]. Conductive polymer hydrogels are a potential candidate to fulfill this need. Their compatibility with biological environments as well as their stretchability and compliance make them ideal for use in applications closely related to humans [1]. However, conductive polymer hydrogels materials tend to be brittle due to their inherent low solid content and poor energy dissipation mechanisms which leads to a low displayed toughness [2]. Ease of fabrication is always a desired trait in any industry. Obtaining an electrically conductive material that is UV-crosslinkable would potentially allow for quick patterning of 2D and 3D complex structures when paired with a Direct Light Patterning (DLP) system, which could be particularly useful for applications where personalized designs are needed [3].

This work focuses on the development of a UV-patternable, strong, conductive, and stretchable hydrogel based on a poly(3,4-ethylenedioxythiophene)-poly(styrenesulfonate) (PEDOT:PSS), poly(vinyl alcohol) methacrylate (PVA-MA), and ionic liquid material system. PEDOT:PSS is a well-known biocompatible conductive polymer with proven solution processability and good conductivity [3]. As shown in Chapter 2.1, the addition of an ionic liquid such as 4-(3-Butyl-1-imidazolio)-1-butanesulfonic acid triflate to a PEDOT:PSS and hydrogel

matrix can potentially improve the composites overall conductivity. In addition to 4-(3-Butyl-1-imidazolio)-1-butanesulfonic acid triflate, this work also utilizes the ionic liquid 1-Ethyl-3-methylimidazolium tricyanomethanide (EMIM TCM) and the ionic liquid 1-Ethyl-3-methylimidazolium trifluoromethanesulfonate (EMIM TFSI). In thin films, several ionic liquids have been utilized to improve conductivity [4, 5] but to our knowledge no such attempt has been made to apply them to conductive hydrogels. Utilizing different ionic liquids can also influence the resulting mechanical properties. Increasing the concentration of the ionic liquid can have a similar effect. Poly(vinyl alcohol) (PVA) is a bio-safe polymer with good mechanical properties and can serve as a strong polymer backbone [6]. By modifying the backbone with a methacrylate derivative (PVA-MA), a photo-polymerizable matrix can be obtained. PVA-MA can be further strengthened by applying different soaking methods which change the structure of the PVA-MA, making it more capable of dissipating fracture energy [7]. The resulting conductive hydrogels can exhibit high strength, considerable stretchability, and good conductivity. With further optimization, this work can potentially be applied as an electrically conductive and conformal material in the development of biomedical devices, soft robots, and hydrogel actuators.

3.2 Materials and Methods

Materials

PEDOT:PSS Clevios™ PH 1000 was acquired from Heraeus with a 1-1.3 wt% PEDOT:PSS solid content. Poly (vinyl alcohol) (PVA), methacrylic acid (MA), hexane, hydrochloric acid, acetone, triethyl amine, 2-Hydroxy-2-methyl-1-phenyl-propan-1-one (Irgacure 1173), and 1-Ethyl-3-methylimidazolium tricyanomethanide (EMIM TCM) were acquired from Fisher Scientific International, Inc. Hydroquinone and 1-Ethyl-3-methylimidazolium

trifluoromethanesulfonate (EMIM TFSI) were purchased from Sigma-Aldrich. 4-(3-Butyl-1-imidazolio)-1-butanesulfonic acid triflate was acquired from Santa Cruz Biotechnology. All chemicals were utilized as received.

Synthesis of PVA-MA

PVA-MA was synthesized via a condensation reaction between PVA, and MA as described in Hua, et al. In brief, 20 grams of PVA are dissolved into 180 mL of DI water in a sealed flask undergoing a water bath at about 90 °C until the PVA was fully dissolved. Next, 40 milligrams of hydroquinone are added to the solution and, once thoroughly mixed, allowed to cool down to room temperature. Once the mixture is cooled down, 5 mL of MA and 10 mL of hydrochloric acid are added into the solution. The mixture was then allowed to stir at about 300 rpm at 60 °C for approximately 12 hours. Once the solution cooled down, 15 mL of triethyl amine are added into the43trengthn. subsequently, the whole mixture was then diluted and precipitated in acetone for 10 cycles. The PVA-MA precipitate is then filtered and dried in vacuum to obtain the final powder.

Fabrication of conductive hydrogel

The UV-curable conductive hydrogel ink was prepared by taking the PEDOT:PSS solution and filtering it with a 0.45μm filter and then vigorously vortexing it before use. PVA-MA was then added in at a 10% (w/v) with respect to the volume of PEDOT:PSS and stirred vigorously within a water bath set to 90 °C until a uniform solution was obtained. Irgacure 1173 constituted the photoinitiator in the ink and was added at a 1% (v/v) with respect to the volume of PEDOT:PSS for all samples. The corresponding ionic liquid was added into the mixture at different concentrations with respect to the volume of PEDOT:PSS solution. Once all if the components

where thoroughly mixed, the mixture was centrifuged to remove any bubbles and the ink was ready poured into a glass slide mold with a 1 mm thickness and exposed to UV light for 300 seconds to ensure complete crosslinking.

Soaking Treatments

After the UV-crosslinking of the conductive hydrogel is completed, it is immersed in DI water for 24 hours to remove any excess reactants. For salting out the gel is then subsequently immersed in 1M Na_2SO_4 for at least 24 hours. For DMSO soak the gel is subsequently immersed in a 60% DMSO/40% water mixture for at least 24 hours. All samples were rinsed with DI water before testing.

Mechanical and electrical testing

To determine the conductive hydrogels electrical properties a hydrogel sample of 30 mm length, 5 mm width and 1 mm thickness was cut out and placed on a four-point electrode array. Based on the obtained resistance and the known dimensions conductivity was calculated via the equation:

$$\sigma = l/RA$$

where l is the length of the hydrogel, A is its cross-sectional area (width times thickness) and R is the resistance. Mechanical testing was done using a Cellscale Unistretch tensile tester with an 8.9N load.

3.3 Results and Discussion

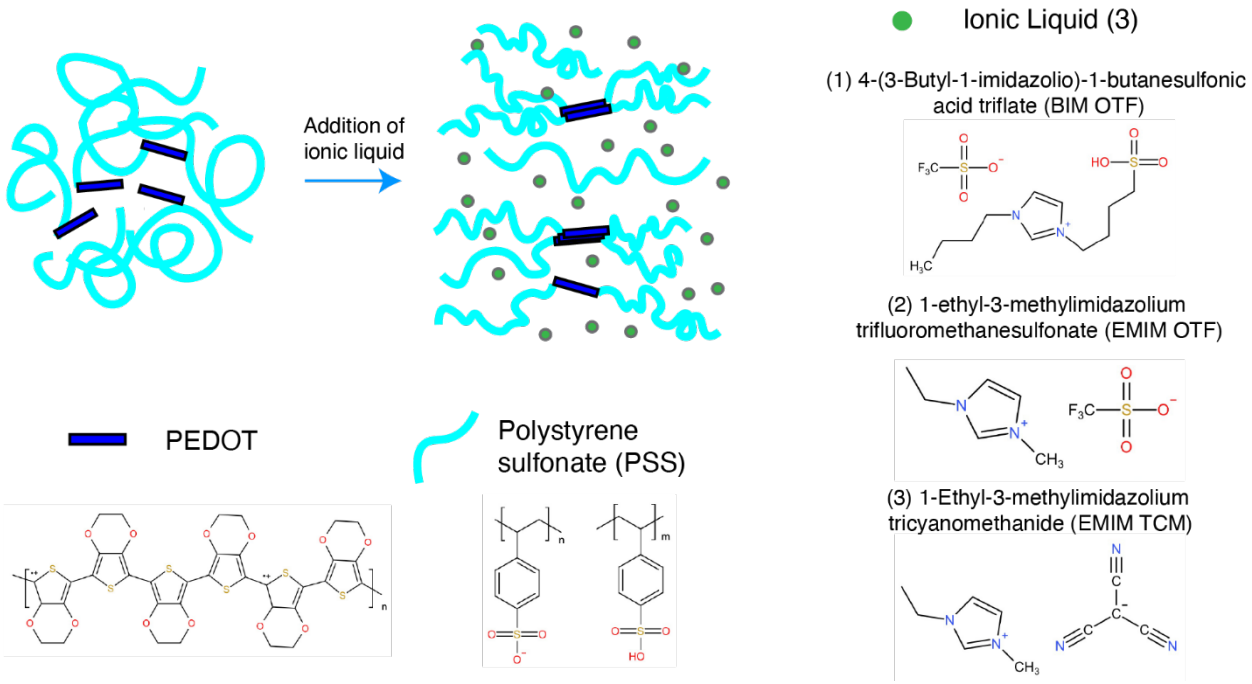

Figure 3.1 PEDOT:PSS and ionic liquid configurational mechanism

The first figures show the mechanisms behind the development of the one-pot synthesis of the strong conductive hydrogel. Pristine PEDOT:PSS exists as small 35 µm globules with the soft PSS chains encasing the hard conductive PEDOT domains and held together by electrostatic interactions between the positively charged PEDOT and negatively charged PSS [8]. Due to this configuration, it is hard for PEDOT domains to encounter each other to form conductive pathways. As shown in Chapter 2.1 of this work and in other published literature [4, 5], ionic liquids can disrupt the interactions between the PEDOT and the PSS domains triggering a configurational change where the PSS chains do not encase the hard PEDOT domains as tightly. This allows the PEDOT domains to encounter each other and become more conductive (Figure 3.1). Even though they exhibit the same overall mechanism, all ionic liquids do not exhibit the same degree of PEDOT:PSS structure disruption which leads to the improvements in conductivity we have come to expect. As previously discussed, ionic liquids consist of a combination of an organic cation and

an organic or inorganic anion whose overall melting point is below 100 °C [9]. The pairing of different anions and cations has proven to result in interesting effects in thin film PEDOT:PSS. In Wu, et al. ionic liquids with the same electrochemically stable cation (1-Ethyl-3-methylimidazolium [EMIM]) but different anions were utilized to develop high-performance PEDOT:PSS-based organic electrochemical transistors. They found that the conductivity largely depended on the electrostatic interactions. The ionic liquid containing a tricyanomethanide (TCM) anion exhibited a higher conductivity than the ionic liquid containing a trifluoromethanesulfonate (OTF) anion [4]. The use of bright-field transmission electron microscopy (TEM) confirmed that EMIM TCM was able to induce thicker PEDOT fibril formation than EMIM OTF. 4-(3-Butyl-1-imidazolio)-1-butanesulfonic acid triflate (BIM OTF) contains the same anion as EMIM OTF paired with a different cation. While all three ionic liquids have been demonstrated in their use as additives for thin film PEDOT:PSS in separate works [4,5], only BIM OTF has been shown for conductive hydrogels [10, 11]. Therefore, these three ionic liquids where selected to induce higher conductivity in PEDOT:PSS-based conductive hydrogels as well as to study the effect different cations and anions will have in a conductive hydrogel application.

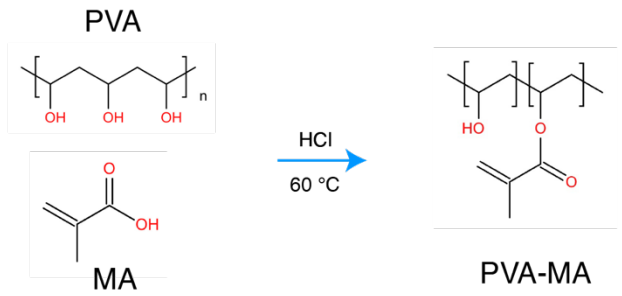

Figure 3.2 PVA and MA condensation reaction to obtain PVA-MA

PVA is a high molecular weight polymer compared to other polymers with similarly short chains which translates into a high fracture energy giving an innate strength. PVA can be crystallized via several methods and these crystallites can serve as physical cross-linking points which further strengthens the hydrogel matrix. PVA-MA is obtained via a condensation reaction between PVA and methacrylic acid (MA) resulting in the partial grafting of methacrylate groups to the PVA backbone (Figure 3.2). The addition of the methacrylate groups allows for the polymer to UV-crosslink which is essential to obtaining a patternable conductive hydrogel. However, their presence also imposes a steric hindrance within the hydrogel matrix and a reduced ability to form crystallites compared to a pure PVA hydrogel and therefore results in a weaker hydrogel [7]. This can be resolved by applying a strengthening treatment to be able to obtain both a patternable, stretchable and strong conductive hydrogel.

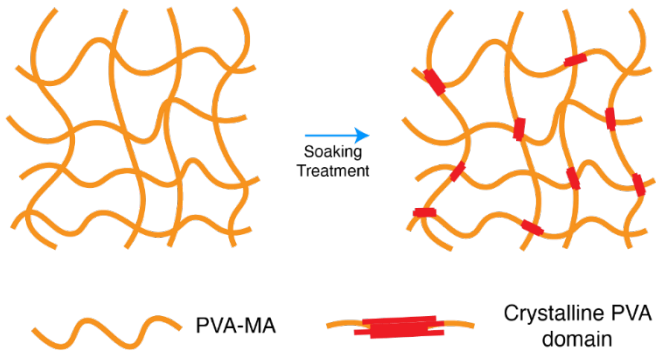

Figure 3.3 Soaking Treatment Mechanism

To improve the mechanical properties of the PVA-MA matrix two strengthening mechanisms were employed. One such method involved strengthening through a DMSO/water cononsolvency effect. This method has already been demonstrated in our group but employed to strengthen freeze-dried PVA anti-freezing hydrogels [12]. Both DMSO and water are miscible in PVA separately, however, in a mixture of PVA, DMSO and water, DMSO and water will prefer

to interact with each other over interacting with the PVA. This results in the formation of hydrogen bonds between the hydroxyl groups that constitute the PVA chain, which act as effective physical crosslinkers and increase the hydrogels' ability to dissipate fracture energy. In other words, the cononsolvency effect between DMSO and water induces crystallization of the PVA chains (Figure 3.3) which leads to a strengthening of the hydrogel. Several papers have found that the ideal DMSO-to-water ratio for this mechanism is 60% DMSO to 40% water so that is what will be utilized [12, 13, 14]. An enhancement of the mechanical properties is not the only benefit a DMSO treatment can provide. Soaking of PEDOT:PSS thin films in DMSO have proven to be an effective way to boost conductivity [15].

The conductivity and mechanical properties of 10% PVA-MA/PEDOT:PSS hydrogel with different ionic liquids added before UV crosslinking and subsequently soaked in DMSO where evaluated (Figure 3.4). As expected, different ionic liquids had a different effect on the overall conductive of the obtained conductive hydrogel. Although they had the same anion, EMIM OTF proved to have a higher conductivity than BIM OTF (Figure 3.5A). Likewise, EMIM TCM had a higher conductivity than EMIM OTF even though they had the same cation (Figure 3.5A).

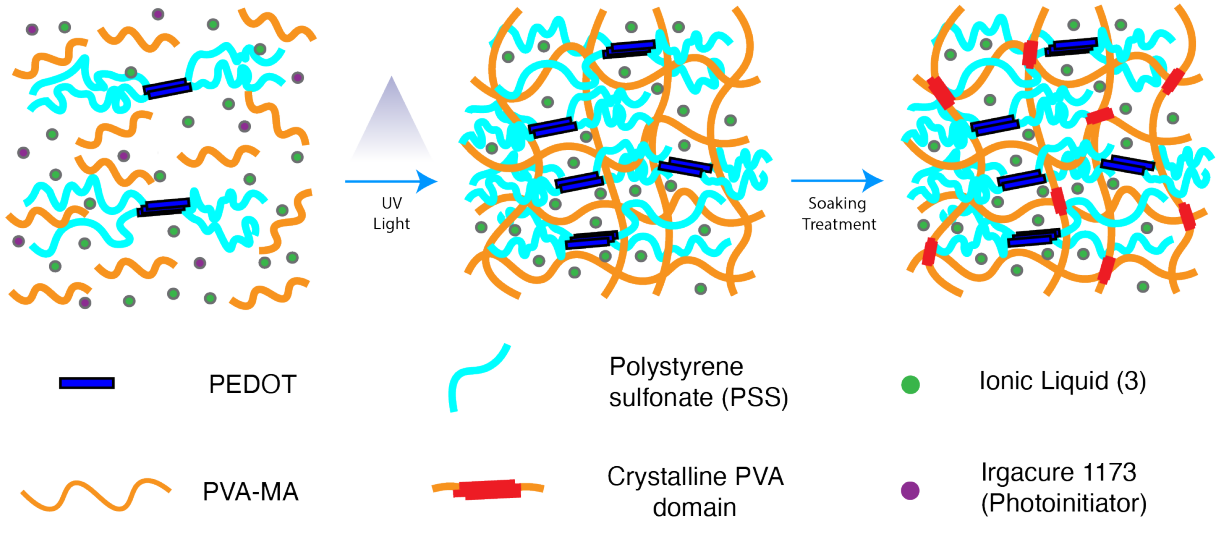

Figure 3.4 Fabrication procedure for the strong, stretchable, and conductive hydrogel

All conductivities where above 10 S/m putting them above other 3D printable conductive hydrogels (Table 2.1). The conductivity trend proves that similarly to the effects seen in PEDOT:PSS thin films, ionic liquid's ability to induce the electrostatic interaction interruptions between PEDOT and PSS that are necessary to achieve a favorable PEDOT domain configuration depends on the combined strengths of both their anion and cation. Although it did not compare the same ionic liquids, the work done by Wang *et al.* to obtain stretchable and conductive PEDOT:PSS thin films alluded to the fact that different ionic liquids can also influence the exhibited mechanical properties [16]. The aggregation of the hard PEDOT domains could potentially not only be increasing the conductivity but also be serving as crosslinking points as well, which leads to an overall stronger conductive hydrogel. Tensile testing seems to corroborate the theory that ionic liquids can both affect the conductivity of PEDOT:PSS within a conductive hydrogel in addition to strengthening the material system as there is a correlation between increased conductivity and increased mechanical properties from the stress-strain curves. BIM OTF exhibited a tensile strength of 1.21 MPa, followed by EMIM OTF with a tensile strength of 1.45 MPa, and finally EMIM TCM with a tensile strength of 1.79 MPa (Figure 3.5B).

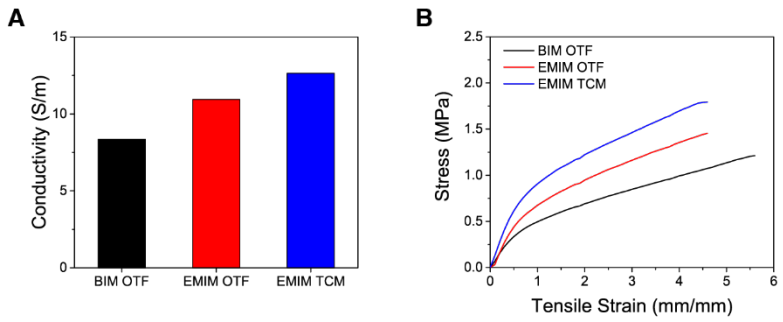

Figure 3.5 A) Conductivity and B) Mechanical properties of DMSO soaked PVA-MA/PEDOT:PSS hydrogels with different ionic liquids

The other strengthening method used in this work was the salting out method, also known as the Hofmeister effect. This method has also already been shown to be useful for this purpose both in PVA [17] and in PVA/(PVA-MA)-g-PNIPAM [7] studies conducted by our research group. Salt anions are capable of polarizing water molecules which leads to the destabilization of the hydrogen bonding that occurs between water and the hydroxyl groups on the PVA chain and promotes reformation of the hydrogen bonds between the hydroxyl groups themselves [17]. This results in crystallization formation (Figure 3.3) which as we know can strengthen PVA hydrogels. Soaking the conductive hydrogels in a 1M Na_2SO_4 solution after subjecting them to a DMSO/water soak resulted in even higher mechanical properties compared to just a DMSO/water soak. BIM OTF exhibited a tensile strength of 2.25 MPa, followed by EMIM OTF with a tensile strength of 2.53 MPa, and finally EMIM TCM with a tensile strength of 2.60 MPa (Figure 3.6B). As for the conductivity, the results showed a similar trend with BIM OTF exhibiting the lowest conductivity, followed by the EMIM OTF, and finally the EMIM TCM (Figure 3.6A). Both strengthening methods resulted in conductive hydrogels with a high conductivity (<10 S/m) and displayed tailorable strong mechanical properties depending on the strengthening method used and on the ionic liquid that was added.

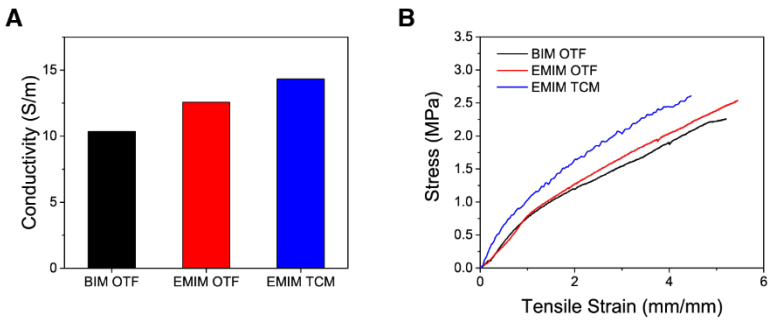

Figure 3.6 A) Conductivity and B) Mechanical properties of DMSO and 1M Na_2SO_4 soaked PVA-MA/PEDOT:PSS hydrogels with different ionic liquids

Table 3.1 Summary of the electrical and mechanical characterization of the conductive hydrogels under the two soaking mechanisms and with different ionic liquids

Soaking Method	Ionic Liquid	Conductivity (S/m)	Tensile Strength (MPa)	Elastic Modulus (MPa)	Strain at Break (%)
DMSO/Water	BIM OTF	8.36	1.21	0.73	560
	EMIM OTF	10.94	1.45	0.96	460
	EMIM TCM	12.64	1.79	1.25	460
DMSO/Water + Salting Out	BIM OTF	10.35	2.25	0.79	520
	EMIM OTF	12.57	2.53	0.81	545
	EMIM TCM	14.33	2.60	1.63	440

Early experiments showed that increasing the concentration of ionic liquid also had a slight effect on both the conductivity and mechanical properties of the material. Samples with different BIM OTF ionic liquid concentration that had gone through both the DMSO/Water and the salting out with 1M Na_2SO_4 were tested. Both tensile strength and an elastic modulus increased with increasing ionic liquid concentration (Table 3.2 and Figure 3.7B). A similar upward trend was observed with the conductivity results (Figure 3.7A). These results suggest that the ionic liquid could have another way of strengthening the conductive hydrogel via interactions with the hydroxyl groups found on the PVA component of the PVA-MA chains themselves. Although not proven with the same ionic liquids used in this work, Fang, *et al.* did find that the more ionic liquid that is added the more the formation of hydrogen bonds between the PVA chains and the ionic liquid is promoted. As hydrogen bonds constitute a physical crosslinking point which can absorb tensile force the resulting hydrogels can exhibit improved mechanical properties [18].

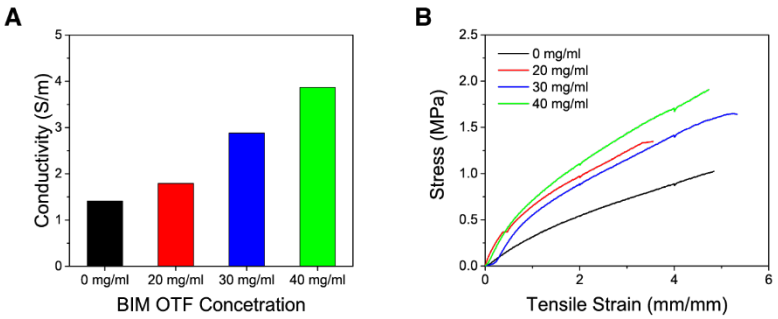

Figure 3.7 A) Conductivity and B) Mechanical properties of DMSO and 1M Na2SO4 soaked PVA-MA/PEDOT:PSS hydrogels with different concentrations of BIM OTF

These results are different in magnitude to the previously shown due to a difference in the batch of PVA-MA utilized. It is believed that this batch was not allowed enough time to go through the condensation reaction and that not enough MA was grafted on to the PVA backbone resulting in the difference in mechanical and conductivity properties. This shows that the PVA-MA is critical to obtaining good mechanical properties and that optimizing its synthesis is required. Regardless, the results still show a general trend which can be utilized for optimization in future work.

Table 3.2 Summary of the electrical and mechanical characterization of the conductive hydrogels with increasing ionic liquids concentrations

Soaking Method	**BIM OTF Concentration**	**Conductivity (S/m)**	**Tensile Strength (MPa)**	**Elastic Modulus (MPa)**	**Strain at Break (%)**
DMSO/Water + Salting Out	0 mg/ml	1.41	1.03	0.31	485
	20 mg/ml	1.79	1.35	0.70	355
	30 mg/ml	2.88	1.65	0.80	530
	40 mg/ml	3.87	1.91	0.91	470

3.4 Conclusion and Future Work

This work demonstrated a one-pot, UV-crosslinkable, conductive hydrogel with high strength and stretchability. A range of conductivities above 10 S/m where successfully obtained, paired with an elastic modulus as high as 1.63 MPa and good strain at break (>150%). Further work would include continued optimization of the ionic liquid species. The three ionic liquids used in this work were chosen for their availability in our lab and their low cost. There are other ionic liquids that have demonstrated higher conductivity when paired with PEDOT:PSS in thin films that have not been characterized in conductive hydrogels. While the obtained elastic modulus is within the range desired for soft robotics (>1 MPa) it is on the lower end. Other strengthening mechanisms such as different salt solutions could be explored. Additionally, utilizing a 3D printing system to fabricate the gel and characterizing the different printing parameters should also be done as well as the realization of 2D and 3D complex structures. Furthermore, a practical demonstration such as a wearable sensor or actuator would need to be done to fully showcase these materials abilities as a strong, stretchable, and conductive hydrogel.

3.5 References

[1] Coyle, S.; Majidi, C.; LeDuc, P.; Hsia, K. J. Bio-inspired soft robotics: Material selection, actuation, and design. *Extreme Mechanics Letters* **2018** *22*, 51–59. https://doi.org/https://doi.org/10.1016/j.eml.2018.05.003

[2] Liu, K.; Wei, S.; Song, L.; Liu, H.; Wang, T. Conductive Hydrogels—A Novel Material: Recent Advances and Future Perspectives. *Journal of Agricultural and Food Chemistry*, **2020** *68*, 7269–7280. https://doi.org/10.1021/acs.jafc.0c00642

[3] Liu, K., Wei, S., Song, L., Liu, H., & Wang, T. Conductive Hydrogels—A Novel Material: Recent Advances and Future Perspectives. *Journal of Agricultural and Food Chemistry* 2020, *68*, 7269–7280. https://doi.org/10.1021/acs.jafc.0c00642

[4] Wu, X.; Stephen, M.; Hidalgo, T. C.; Salim, T.; Surgailis, J.; Surendran, A.; Su, X.; Li, T.; Inal, S.; Leong, W. L. Ionic-Liquid Induced Morphology Tuning of PEDOT:PSS for High-Performance Organic Electrochemical Transistors. *Adv. Funct. Mater.* **2022**, *32*, 2108510. https://doi.org/10.1002/adfm.202108510

[5] Kee, S.; Kim, N.; Kim, B. S.; Park, S.; Jang, Y. H.; Lee, S. H.; Kim, J.; Kim, J.; Kwon, S.; Lee, K. Controlling Molecular Ordering in Aqueous Conducting Polymers Using Ionic Liquids. *Advanced Materials*, **2016** *28*, 8625‑8631. https://doi.org/10.1002/adma.201505473

[6] Li, J.; Suo, Z.; Vlassak, J. J. Stiff, strong, and tough hydrogels with good chemical stability. *J. Mater. Chem. B* **2014**, *2*, 6708–6713. https://doi.org/10.1039/C4TB01194E

[7] Hua, M.; Wu, D.; Wu, S.; Ma, Y.; Alsaid, Y.; He, X. 4D Printable Tough and Thermoresponsive Hydrogels. *ACS Applied Materials & Interfaces* **2021,** *13*, 12689–12697. https://doi.org/10.1021/acsami.0c17532

[8] Kayser, L. v.; Lipomi, D. J. Stretchable Conductive Polymers and Composites Based on PEDOT and PEDOT:PSS. *Advanced Materials* **2019**, *31*, 1–13. https://doi.org/10.1002/adma.201806133.

[9] Zhou, T., Gao, X., Dong, B., Sun, N., & Zheng, L. Poly(ionic liquid) hydrogels exhibiting superior mechanical and electrochemical properties as flexible electrolytes. *J. Mater. Chem. A* **2016**, *4*(3), 1112–1118. https://doi.org/10.1039/C5TA08166A

[10] Feig, V. R.; Tran, H.; Lee, M.; Bao, Z. Mechanically Tunable Conductive Interpenetrating Network Hydrogels That Mimic the Elastic Moduli of Biological Tissue. *Nature Communications* **2018**, *9*, 1–9. https://doi.org/10.1038/s41467-018-05222-4.

[11] Liu, Y.; Liu, J.; Chen, S.; Lei, T.; Kim, Y.; Niu, S.; Wang, H.; Wang, X. Foudeh, A. M.; Tok, J. B.-H.; Bao, Z. Soft and elastic hydrogel-based microelectronics for localized low-voltage neuromodulation. *Nat. Biomed. Eng.* **2019,** *3***,** 58–68. https://doi.org/10.1038/s41551-018-0335-6

[12] Wu, S, Alsaid, Y, Yao, B, et al. Rapid and scalable fabrication of ultra-stretchable, anti-freezing conductive gels by cononsolvency effect. *EcoMat*. **2021**, 3, e12085. https://doi.org/10.1002/eom2.12085

[13] Kanaya, T.; Takahashi, N.; Takeshita, H.; Ohkura, M.; Nishida, K.; Kaji, K. Structure and dynamics of poly(vinyl alcohol) gels in mixtures of dimethyl sulfoxide and water. *Polym. J.* **2012,** *44,* 83–94. https://doi.org/10.1038/pj.2011.88

[14] Takahashi, N., Kanaya, T., Nishida, K., & Kaji, K. Effects of cononsolvency on gelation of poly(vinyl alcohol) in mixed solvents of dimethyl sulfoxide and water. *Polymer* **2003,** *44*, 4075–4078. https://doi.org/https://doi.org/10.1016/S0032-3861(03)00390-2

[15] Lingstedt, L. V.; Ghittorelli, M.; Lu, H.; Koutsouras, D. A.; Marszalek, T.; Torricelli, F.; Crăciun, N. I.; Gkoupidenis, P.; Blom, P. W. M. Effect of DMSO Solvent Treatments on the Performance of PEDOT:PSS Based Organic Electrochemical Transistors. *Adv. Electron. Mater.* **2019**, *5*, 1800804. https://doi.org/10.1002/aelm.201800804

[16] Wang, Y.; Zhu, C.; Pfattner, R.; Yan, H.; Jin, L.; Chen, S.; Molina-Lopez, F.; Lissel, F.; Liu, J.; Rabiah, N. I.; Chen, Z.; Chung, J. W.; Linder, C.; Toney, M. F.; Murmann, B.; Bao, Z.

A Highly Stretchable, Transparent, and Conductive Polymer. *Science Advances* **2017**, *3*, 1–11. https://doi.org/10.1126/sciadv.1602076

[17] Wu, S.; Hua, M.; Alsaid, Y.; Du, Y.; Ma, Y.; Zhao, Y.; Lo, C.-Y.; Wang, C.; Wu, D.; Yao, B.; Strzalka, J.; Zhou, H.; Zhu, X.; He, X. Poly(vinyl alcohol) Hydrogels with Broad-Range Tunable Mechanical Properties via the Hofmeister Effect. *Adv. Mater*. **2021**, *33*, 2007829. https://doi.org/10.1002/adma.202007829

[18] Fang, H.; Wang, J.; Li, L.; Xu, L.; Wu, Y.; Wang, Y.; Fei, X.; Tian, J.; Li, Y. A novel high-strength poly(ionic liquid)/PVA hydrogel dressing for antibacterial applications. *Chem. Eng. J.* **2019,** *365*, 153–164. https://doi.org/https://doi.org/10.1016/j.cej.2019.02.030

Chapter 4: Conclusion and Outlook

This thesis focused on the development of printable one-pot synthesis conductive hydrogel inks. The realization of conductive hydrogels that are patternable, stretchable (>150%) and that exhibit high conductivity (> 2 S/m) is still hard to achieve simultaneously. Two different mechanical property ranges where targeted in this work: soft and tissue like in the 1-100 kPa elastic modulus range and stronger properties above the 1 MPa elastic modulus range. Leveraging the conductivity of PEDOT:PSS enhanced by the addition of ionic liquids and the mechanical properties provided by either PAAm or PVA-MA, both systems where able to achieve higher conductivity (>10 S/m) than any previous 3D printable and stretchable (>150%) materials found in literature.

In future work, being able to prove cell seeding with these material systems would be a good way to showcase their biocompatibility using the material system developed in Chapter 2. This work proved the ability of ionic liquids to modify the structure of PEDOT:PSS to increase its conductivity through direct addition into the material system. There are other ionic liquids that have demonstrated higher conductivity when paired with PEDOT:PSS in thin films that have not been characterized in conductive hydrogels which could prove to be useful to obtaining tunable mechanical and conductive properties for these systems. It's possible that soaking with ionic liquids could be another potential avenue to increasing conductivity in the material system developed in Chapter 3, however, ionic liquids are expensive to purchase in large quantities. Developing in-house capabilities to synthesize ionic liquids could potentially circumvent this problem.